An ensemble based on a bi-objective evolutionary spectral algorithm for graph clustering

Camila P.S. Tautenhain[a], Mariá C.V. Nascimento[a,*]

[a]*Instituto de Ciência e Tecnologia, Universidade Federal de São Paulo*
São José dos Campos, Brazil

Abstract

Graph clustering is a challenging pattern recognition problem whose goal is to identify vertex partitions with high intra-group connectivity. This paper investigates a bi-objective problem that maximizes the number of intra-cluster edges of a graph and minimizes the expected number of inter-cluster edges in a random graph with the same degree sequence as the original one. The difference between the two investigated objectives is the definition of the well-known measure of graph clustering quality: the modularity. We introduce a spectral decomposition hybridized with an evolutionary heuristic, called *MOSpecG*, to approach this bi-objective problem and an ensemble strategy to consolidate the solutions found by *MOSpecG* into a final robust partition. The results of computational experiments with real and artificial LFR networks demonstrated a significant improvement in the results and performance of the introduced method in regard to another bi-objective algorithm found in the literature. The crossover operator based on the geometric interpretation of the modularity maximization problem to match the communities of a pair of individuals was of utmost importance for the good performance of *MOSpecG*. Hybridizing spectral graph theory and intelligent systems allowed us to define significantly high-quality community structures.

Keywords: Graph clustering, Community detection, Evolutionary heuristic, Multi-objective optimization, Modularity maximization, Spectral decomposition

1. Introduction

The majority of graphs that describe real networks, such as social and metabolic networks (Zachary, 1977; Lancichinetti et al., 2011), are characterized by vertex partitions with high

*Corresponding author.
Email addresses: `santos.camila@unifesp.br` (Camila P.S. Tautenhain), `mcv.nascimento@unifesp.br` (Mariá C.V. Nascimento)

intra-cluster connectivity (Girvan & Newman, 2002). The graph clustering problem, also known as community detection problem, aims at finding such partitions. Ferrara et al. (2014), for example, developed an expert system to detect communities in mobile phone networks formed by interactions of criminals to possibly identify criminal organizations. Larsson & Moe (2012) and Golbeck et al. (2010) applied community detection algorithms to Twitter data to classify the users' political leaning. In practice, this type of information usually benefits political campaigners.

The formal definition of a graph clustering problem leans towards the criterion to assess the partitioning quality. Examples of optimization criteria to finding graph clusterings are the maximization of modularity (Newman & Girvan, 2004), the map equation minimization (Rosvall & Bergstrom, 2008) and the maximization of the statistical significance of communities according to the measure introduced by Lancichinetti et al. (2011). In particular, the map equation measure is based on the observation on the duality between graph clustering problems and the data compression problem described by the minimization of the path length of a random walker. The Infomap algorithm was then proposed to detect communities that minimize the map equation. Lancichinetti et al. (2011) studied a measure that evaluates the statistical significance of the communities in a network by calculating their probability of existing in a random graph with the same degree sequence as the original one. The authors introduced a solution method to find a partitioning of the vertices that maximizes these probabilities named Order Statistics Local Optimization Method (OSLOM).

Despite Infomap and OSLOM being considered state-of-the-art methods, the optimization criteria they employ have not been properly explored by other algorithms yet. Modularity maximization, on the other hand, is one of the most popular optimization criteria to define graph clusterings. The modularity of a partition is the difference between the number of edges in the same groups (first term) and the expected number of edges within the groups in a random graph with the same vertex degree sequence as the original graph (second term) (Newman & Girvan, 2004). However, many studies in the literature point out that by simply defining the measure as the difference between these two terms, without scaling them, may be a poor way to evaluate graph clusterings (Fortunato & Barthélemy, 2007; Reichardt & Bornholdt, 2006).

As an attempt to mitigate the scaling problem of modularity, Reichardt & Bornholdt (2006) suggested multiplying the second term of the modularity measure by a parameter called resolution parameter. A few studies approaching this modified modularity have shown interesting results (Santos et al., 2016; Carvalho et al., 2014). Carvalho et al. (2014), for example, introduced a supervised method that automatically adjusts the resolution parameter based on the graph topology. The method was later employed in the consensus algorithm proposed by Santos et al. (2016). In spite of the potential of the strategies, they require la-

beled data for defining a training set of the supervised algorithm. Berry et al. (2011); De Meo et al. (2013) and Khadivi et al. (2011) introduced pre-processing strategies to change the edge weights of a graph in order to diminish the negative effects of the resolution limit without the prior knowledge of the resolution parameter.

Another approach that explores the duality between the first and second terms of the modularity measure was introduced by Shi et al. (2012). The authors introduced an evolutionary algorithm called MOCD for solving the bi-objective problem that maximizes the first term of modularity and minimizes the second term of modularity. The studies in (Pizzuti, 2012; Gong et al., 2012, 2014) also investigate bi-objective problems by optimizing different criteria. In particular, MOCD achieved good quality partitions when compared to the other evolutionary bi-objective clustering algorithm, known as Moga-Net (Pizzuti, 2012).

This paper investigates a weighted aggregation method for solving the bi-objective problem that optimizes the first and second terms of modularity. The resulting problem is here called weighted aggregate modularity and is equivalent to solving the problems that maximize the modularity with different resolution parameter values, as demonstrated in this paper. To solve the weighted aggregate modularity, we propose a multi-objective evolutionary algorithm whose fitness function is the spectral relaxation of the weighted aggregate modularity matrix. In addition, we explore the close relationship between multi-objective clusterings and ensemble clusterings by introducing an ensemble of the approximation of the Pareto solutions that adjusts the edge weights of the graph. To the best of our knowledge, ensemble or consensus clustering strategies have not been applied to solutions of the studied bi-objective graph clustering problem. The proposed algorithm deals with the resolution limit by combining both the edge weighting and resolution parameter strategies, without the need of pre-defining the resolution parameter. Furthermore, we estimate an upper bound to the number of clusters in advance, which might contribute to further reductions of the negative effects of the resolution limit according to the computational experiments performed by Darst et al. (2014).

Computational experiments were carried out using real and LFR networks (Lancichinetti et al., 2008). We contrasted the results achieved by the proposed algorithm with those found by Moga-Net, a reference multi-objective method. Moreover, we compared the results with OSLOM and Infomap. The proposed algorithm outperformed the multi-objective algorithm Moga-Net in all the networks and was from 6 to 64 times faster in the LFR networks. Despite the slightly better results achieved by the reference mono-objective algorithms OSLOM (Lancichinetti et al., 2011) and Infomap (Rosvall & Bergstrom, 2008) in most of the LFR networks, the proposed algorithm outperformed them in the LFR networks with large mixture coefficients.

The rest of this paper is organized as follows: Section 2 presents a brief literature review

of multi-objective and ensemble graph clustering algorithms; Section 3 thoroughly describes the studied spectral decomposition of the weighted aggregate modularity; Section 4 introduces the multi-objective evolutionary algorithm proposed in this paper; Section 5 discusses the computational experiments carried out with the algorithm in question along with the analysis of the results; and, to sum up, Section 6 brief summarizes the contributions of the paper and outlines further works.

2. Related Works

This section presents a concise literature review focusing on multi-objective optimization and consensus clustering. As earlier mentioned, both types of strategies are approached in this paper to mitigate the bias of algorithms that optimize a single quality measure.

2.1. Multi-objective graph clustering methods

Multi-objective optimization involves solving problems with two or more conflicting objective functions. The existence of trade-offs amongst objective functions is the reason why a single solution cannot optimize all the functions simultaneously; instead, a number of efficient solutions, known as Pareto solutions, describes the best solutions for adequate decision-making. In a multi-objective problem, a solution is called efficient when it is not possible to improve the value of any objective function without worsening the value of another function.

Because of the computational challenges involved in graph partitioning problems, especially in large-scale networks, the existing multi-objective solution methods are heuristics. In particular, the overwhelming majority of multi-objective graph clustering solution methods are evolutionary algorithms (Pizzuti, 2012; Gong et al., 2012; Shi et al., 2012; Amiri et al., 2013; Shang et al., 2016; Žalik & Žalik, 2018; Cheng et al., 2018; Zou et al., 2019), due to the set of evolved solutions provided by their population-based structure. Methods based on particle swarm optimization (Gong et al., 2014; Chen et al., 2016; Pourkazemi & Keyvanpour, 2017; Rahimi et al., 2018) and other nature- or human-inspired algorithms (Gong et al., 2011; Li et al., 2012; Gong et al., 2013; Xu et al., 2015; Zhou et al., 2016; Amiri et al., 2011; Amiri et al., 2013) were also proposed to solve multi-objective graph clustering problems.

2.1.1. Optimization of the modularity terms

As mentioned in the earlier section of this paper, Shi et al. (2012) introduced MOCD to optimize the two terms of the modularity measure. Li et al. (2012) and Žalik & Žalik (2018) also optimized the two terms of the modularity measure using multi-objective evolutionary algorithms.

For this, Li et al. (2012) applied a multi-objective harmony search clustering algorithm called SCAH-MOHSA to the matrix of eigenvectors of the normalized adjacency matrix. It is worth pointing out that Li et al. (2012) have suggested a spectral-based algorithm. This strategy of detecting communities in networks by finding clusters in an eigenvector matrix which is the solution of the spectral relaxation of graph partitioning problems is widely employed in the literature. However, clustering algorithms based on this strategy are known to not scale well since they work with a non-sparse matrix. In this context, there is a dearth in the literature on efficient spectral-based methods to optimize multi-objective graph clustering problems.

Žalik & Žalik (2018) introduced CM-Net as a combination of problem-specific genetic operators with a multi-objective algorithm based on the Non-dominated Sorting Genetic Algorithm II (NSGA-II) (Deb et al., 2002). SCAH-MOHSA and CM-Net outperformed an algorithm found in the literature – known as Moga-Net, which is discussed in the next section – in artificial networks proposed by (Girvan & Newman, 2002). On the one hand, both SCAH-MOHSA and CM-Net found partitions with higher modularity values than Moga-Net in real networks. On the other hand, when contrasting the partitions obtained by SCAH-MOHSA and by Moga-Net with the expected partitions, the algorithms were competitive[1].

In the next section, we briefly present studies about multi-objective graph clustering algorithms that employ criteria different from modularity to optimize.

2.1.2. Other optimization criteria

Pizzuti (2009, 2012) introduced a bi-objective genetic algorithm, also based on NSGA-II, which the authors named Moga-Net, to detect communities by maximizing the so-called community score (Pizzuti, 2008) and minimizing a function named community fitness (Lancichinetti et al., 2008). On the one hand, the community score is based on the evaluation of the number of edges inside communities. On the other, the community fitness relies on the assessment of the number of edges between vertices from different communities. In computational experiments with large real networks, the modularity values of the best modularity valued partitions from the Pareto sets found by Moga-Net were worse than those found by a mono-objective spectral clustering algorithm in the literature. The studies performed in (Gong et al., 2011; Amiri et al., 2011, 2012; Amiri et al., 2013) approached the same bi-objective problem and presented heuristic methods competitive with Moga-Net.

Gong et al. (2012) suggested a bi-objective problem that aims at maximizing the ratio association (Angelini et al., 2007) and minimizing the ratio cut (Wei & Cheng, 1991).

---

[1]Žalik & Žalik (2018) did not contrast the partitions obtained by CM-Net with the expected partitions.

The ratio association and ratio cut assess the sum of the internal and external degrees, respectively, of the subgraphs induced by the communities of the graph. Both measures are normalized by the number of vertices in each community. Other authors also studied these measures in the literature e.g. in (Zhou et al., 2016; Chen et al., 2016; Shang et al., 2016; Pourkazemi & Keyvanpour, 2017; Zou et al., 2017; Cheng et al., 2018; Zhu et al., 2008).

2.1.3. Solution selection for the decision-making

It is worth mentioning that solution selection strategies can be used in applications which require a single solution from multi-objective community detection algorithms that return a Pareto set approximation. One of the most common strategies is to select from the set the partition with the highest modularity value (Pizzuti, 2009, 2012; Shi et al., 2012; Gong et al., 2012, 2013; Ghaffaripour et al., 2016; Pourkazemi & Keyvanpour, 2017). Shi et al. (2012), in addition to this strategy, suggested considering the minimum standard deviation of the Pareto solutions from those obtained to a graph generated randomly with the same degree sequence as the graph under study. The selected Pareto solution is the one whose minimum standard deviation is the largest among all Pareto solutions. Žalik & Žalik (2018) suggested ranking the partitions according to their non-domination level measured by the crowding distance, as suggested in NSGA-II.

Another form to return a single partition from a given set of solutions is by consensus clustering strategies. Kanawati (2015) suggested using different consensus and ensemble strategies to obtain a partition from outputs of a graph clustering algorithm. Nevertheless, the method of Kanawati (2015) was designed only to find clusters of target nodes in a distributed form. In this paper, we propose a consensus strategy to define a partition from the Pareto solutions, instead of employing the measure-based strategies introduced in the literature that are biased to a single evaluation metric. By using the consensus clustering, our goal is to capture the core communities of the Pareto set and to weight the joint relation between vertices to define their final communities.

In this context, the next section briefly reviews ensemble and consensus clustering methods for graph clustering.

2.2. Consensus clustering

Ensemble and consensus clustering are both solution methods that combine algorithms, partitions or models to perform the clustering task. These methods have been intensively studied in the last decades (Nascimento et al., 2009; Lancichinetti & Fortunato, 2012; Santos et al., 2016). They tend to be more robust than those that optimize a single criterion.

The ensemble algorithms for graph clustering related to the study performed in this paper belong to the class of consensus methods that combines partitions from a set of diverse partitions in order to determine a consensus partition. The strategy to define such

consensus partitions relies on observing whether a pair of vertices is in the same group in most of the partitions in the set. Studies (Lancichinetti & Fortunato, 2012), (Liang et al., 2014) and (Santos et al., 2016) obtained good results using these methods.

The consensus strategy proposed by Lancichinetti & Fortunato (2012) achieved better results than ensemble algorithms based on the modularity maximization using the majority rule. Liang et al. (2014) combined a consensus strategy with a label propagation (LP) algorithm (Raghavan et al., 2007) to obtain better partitions than LP. As previously mentioned, although Kanawati (2015) approached a graph clustering problem which does not find a partitioning, one of the strategies the author employed is founded on the definition of a consensus matrix, similar to the strategy that we introduce in this paper.

In their consensus clustering, Santos et al. (2016) identified a consensual partition from a set of partitions obtained by an algorithm that aims to maximize the modularity adjusted for different values of the resolution parameter. The consensual partition is obtained by assigning the same community to vertices that are in the same community on at least half of the partitions of the set.

3. Weighted Aggregate Modularity

This section discusses the spectral decomposition of the weighted aggregate modularity. Throughout this paper, let $G = (V, E)$ be an undirected graph, where V is its set of n vertices and E is its set of m edges. The edges of G are unordered pairs of distinct adjacent vertices (i, j), where $i, j \in V$. Let $A = [a_{ij}] \in \mathbb{N}^{n \times n}$ be the adjacency matrix of G, i.e., a_{ij} is 1 if $(i, j) \in E$, and 0 otherwise. The degree of a vertex i, d_i, is given by $\sum_{j \in V} a_{ij}$. A vertex partition with k clusters (groups or communities) is here defined as $P = \{C_1, C_2, \ldots, C_k\}$, where $\bigcup_{t=1}^{k} C_t = V$ and $C_t \cap C_{t'} = \emptyset$, $\forall t \neq t' \in \{1, 2, \ldots, k\}$. The label of a cluster C_t is t and, for ease of notation, we refer to cluster C_t as the cluster with label t and to the label of the cluster of a vertex i in a partition P as $\mathcal{C}_P(i)$.

Modularity is a measure that assesses the difference between the number of edges within clusters and its expected number in a random graph with the same degree sequence as the graph under consideration. Equation (1) presents a way to calculate the modularity measure originally introduced by Newman & Girvan (2004).

$$Q(P) = \frac{1}{2m} \sum_{i,j \in V} \left(a_{ij} - \frac{d_i d_j}{2m} \right) \delta_{\mathcal{C}_P(i), \mathcal{C}_P(j)} \tag{1}$$

In Equation (1), $\delta_{\mathcal{C}_P(i), \mathcal{C}_P(j)}$ is an indicator function that assumes value 1 if $\mathcal{C}_P(i) = \mathcal{C}_P(j)$, and 0 otherwise. The resolution parameter, as suggested by Reichardt & Bornholdt (2006), is a scalar γ that multiplies the term $\frac{d_i d_j}{2m}$ in Equation (1).

Equation (1) shows that in order to maximize the modularity, the first term, i.e. a_{ij}, must be maximized and the second term, i.e. $\frac{d_i d_j}{2m}$, has to be minimized. On the one hand, the higher the number of edges within clusters, the higher the first term. On the other, the lower the number of edges within clusters, the lower the expected number of edges within clusters and consequently, the lower the second term. These two terms, therefore, are conflicting and result in a trade-off in the modularity measure (Brandes et al., 2008).

As discussed earlier in this paper, Shi et al. (2012) have approached the bi-objective problem that optimizes the two terms of modularity. Equations (2) and (3) present the pair of objective functions of the bi-objective problem.

$$\max_P Q^{IN}(P) = \frac{1}{2m} \sum_{i,j \in V} a_{ij} \delta_{\mathcal{C}_P(i), \mathcal{C}_P(j)} \tag{2}$$

$$\min_P Q^{NULL}(P) = \frac{1}{2m} \sum_{i,j \in V} \frac{d_i d_j}{2m} \delta_{\mathcal{C}_P(i), \mathcal{C}_P(j)} \tag{3}$$

Consider the weighted aggregation of the objective functions $Q^{IN}(P)$ and $Q^{NULL}(P)$ as presented in Equation (4). The objective function (3) can be transformed into a maximization function without loss of generality by multiplying the function by -1.

$$QW(P) = \frac{1}{2m} \sum_{i,j \in V} \left[\gamma_1 a_{ij} - \gamma_2 \frac{d_i d_j}{2m} \right] \delta_{\mathcal{C}_P(i), \mathcal{C}_P(j)}, \tag{4}$$

where $\gamma_1, \gamma_2 \in \mathbb{R}, \gamma_1 + \gamma_2 = 1$.

The set of solutions for the weighted aggregation problem for different values of γ_1 and γ_2 are efficient (Ehrgott, 2005), and thereby provide an approximation to the Pareto frontier of the bi-objective problem. Moreover, as γ_1 and γ_2 are both scalars, when $\gamma_1 > 0$ the optimization problem $\max_P QW$ is equivalent to $\frac{1}{\gamma_1} \max_P QW$, which is exactly the adjusted modularity maximization problem. Therefore, the solutions of the modularity maximization problem with different values of resolution parameter are also efficient Pareto solutions for the bi-objective problem (2)-(3). In particular, the maximization of Equation (4) for $\gamma_1 = \gamma_2 = 0.5$ is equivalent to the classical modularity maximization problem.

We also say that a partition P_a dominates a partition P_b if and only if $Q^{IN}(P_a) > Q^{IN}(P_b)$ and $Q^{NULL}(P_a) \leq Q^{NULL}(P_b)$ or if and only if $Q^{IN}(P_a) \geq Q^{IN}(P_b)$ and $Q^{NULL}(P_a) < Q^{NULL}(P_b)$.

3.1. Spectral decomposition

This section presents the spectral decomposition of the weighted aggregation of modularity provided in Equation (4). It is strongly based on the spectral decomposition proposed

by Newman (2006). Let us first define in Equation (5) the weighted aggregate matrix $BW = [bw_{ij}] \in \mathbb{R}^{n \times n}$.

$$bw_{ij} = \gamma_1 a_{ij} - \gamma_2 \frac{d_i d_j}{2m} \tag{5}$$

Note that the modularity matrix is $B = \frac{1}{\gamma_1} BW$, where $\gamma = \frac{\gamma_2}{\gamma_1} = 1$. Consider the sequence of eigenvalues of matrix BW, $\lambda_1, \lambda_2, \ldots, \lambda_n$, sorted in the decreasing order of absolute value, that is, $|\lambda_1| \geq |\lambda_2| \geq \cdots \geq |\lambda_n|$. Let $U \in \mathbb{R}^{n \times n}$ be a matrix such that its j-th column, referred to as column u_j, is an eigenvector of BW associated with eigenvalue λ_j. BW is symmetric and thus admits an eigen-decomposition: $BW = U \Lambda U^T$, where $\Lambda = [\Lambda_{ij}] \in \mathbb{R}^{n \times n}$ is a diagonal matrix such that $\Lambda_{ii} = \lambda_i$.

Let $S = [s_{it}] \in \mathbb{N}^{n \times k}$ be a binary matrix associated with a solution of the graph clustering problem. Element s_{it} receives 1 if vertex i belongs to cluster C_t, and 0 otherwise. Therefore, $\delta_{\mathcal{C}_P(i),\mathcal{C}_P(j)} = \sum_{t=1}^{k} s_{it} s_{jt}$. Equation (4) can hence be rewritten as indicated in Equation (6).

$$QW(P) = \frac{1}{2m} \sum_{i,j \in V} \sum_{t=1}^{k} bw_{ij} s_{it} s_{jt} = \frac{1}{2m} Tr(S^T BW S) \tag{6}$$

Any given vertex belongs to exactly and only one cluster, which implies that $\sum_{t=1}^{k} s_{it} = 1, i = 1, \ldots, n$, and $Tr(S^T S) = n$. Knowing that U is an orthogonal matrix, we can rewrite Equation (6) as Equation (7).

$$QW(P) = \frac{1}{2m} Tr[S^T U \Lambda U^T S] = \frac{1}{2m} \sum_{j=1}^{n} \sum_{t=1}^{k} \lambda_j (\sum_{i=1}^{n} u_{ij} s_{it})^2 \tag{7}$$

Since Equation (7) shows that only positive eigenvalues increase the value of QW, Newman (2006) suggested approximating Equation (7) using only the first largest positive eigenvalues. Nonetheless, Newman (2006) also demonstrated that negative eigenvalues are important to indicate vertices that decrease the $QW(P)$ in case they are clustered together. This paper takes into account the negative eigenvalues by selecting the first p eigenvalues sorted in decreasing order of absolute value.

Consider $\mathcal{E}$ the set of the first p eigenvalues of BW; let $\mathcal{E}p = \{j | \lambda_j \in \mathcal{E}$ such that $\lambda_j \geq 0\}$ and $\mathcal{E}n = \{j | \lambda_j \in \mathcal{E}$ such that $\lambda_j < 0\}$ be the positive and negative eigenvalue indices, respectively. Moreover, let $rp^i \in \mathbb{R}^p$ and $rn^i \in \mathbb{R}^p$ be the vectors regarding vertex i whose components are defined by Equations (8) and (9), respectively. Also, in this paper, rp^i is called positive vector of vertex i, whereas rn^i is referred to as negative vector of vertex i.

$$rp_j^i = \begin{cases} \sqrt{\lambda_j} u_{ij} & , \text{ if } j \in \mathcal{E}_p \\ 0 & , \text{ if } j \in \mathcal{E}_n \end{cases} \tag{8}$$

$$rn_j^i = \begin{cases} \sqrt{-\lambda_j}u_{ij} & , \text{ if } j \in \mathcal{E}_n \\ 0 & , \text{ if } j \in \mathcal{E}_p \end{cases} \tag{9}$$

Equation (10) approximates Equation (7) using the p largest eigenvalues in absolute value.

$$\begin{aligned} QW(P) &\simeq \frac{1}{2m} \sum_{\lambda_j \in \mathcal{E}} \sum_{t=1}^k \left[\sum_{i=1}^n \sqrt{|\lambda_j|} u_{ij} s_{it} \right]^2 \\ &= \frac{1}{2m} \sum_{t=1}^k \sum_{j=1}^p \left[\left(\sum_{i \in C_t} rp_j^i \right)^2 - \left(\sum_{i \in C_t} rn_j^i \right)^2 \right] \\ &= \frac{1}{2m} \sum_{t=1}^k (||Rp^t||^2 - ||Rn^t||^2) \end{aligned} \tag{10}$$

where $\forall j \in \{1, \ldots, p\}$, $Rp_j^t = \sum_{i \in C_t} rp_j^i$ and $Rn_j^t = \sum_{i \in C_t} rn_j^i$.

Furthermore, $Rp^t = [Rp_j^t]_{j=1\ldots p}$ and $Rn^t = [Rn_j^t]_{j=1\ldots p}$ are referred to as vectors of cluster C_t. In this paper, Rp^t is called positive vector of cluster C_t, whereas Rn^t is referred to as negative vector of cluster C_t.

Similarly to the results of the approximation with positive eigenvalues carried out by Newman (2006), we have reduced the weighted aggregate modularity maximization problem into a vector partitioning problem. The goal of the vector partitioning problem is to find a vertex partition by maximizing the terms Rp^t and minimizing the terms Rn^t, for $t = 1, 2, \ldots, k$.

It is well-known that the number of groups has a direct impact on the number of eigenvectors required to determine graph clusterings. Thereby, most spectral heuristics must first define the number of groups, which is generally not known in advance.

3.2. Defining the number of clusters

In this paper, we adapted the strategy to identify the number of clusters presented by Krzakala et al. (2013), who constructed a matrix called non-backtracking matrix from the adjacency matrix of a given graph and estimated the number of clusters through the eigenvalues of this matrix.

The adaptation proposed here consists in estimating the number of clusters based on the weighted aggregate modularity matrix BW. Let χ be the largest (leading) eigenvalue of BW. The proposed algorithm sets k' as the number of eigenvalues of BW higher than $\sqrt{\chi}$. In this paper, we estimate the number of clusters, k, to be $\lfloor 1.25k' \rfloor$. This estimation is an

upper bound to the number of clusters because the proposed algorithm might leave one or more clusters empty.

Figure 1 displays an example of the proposed strategy by depicting the eigenvalues of the Karate network (Zachary, 1977), whose largest eigenvalue is 4.977. The red squares in this figure indicate the points $(-\sqrt{\chi}, 0)$ and $(\sqrt{\chi}, 0)$ and a circumference of radius $\sqrt{\chi}$ centered at the origin of the Cartesian plane. Most of the black dots, which correspond to the eigenvalues of matrix BW, are enclosed by the circumference. The proposed algorithm estimates k' to be the number of eigenvalues higher than $\sqrt{\chi}$, i.e., the number of positive points outside the circumference, which is 3. Therefore, the upper bound estimation to the number of clusters is $k = 3$.
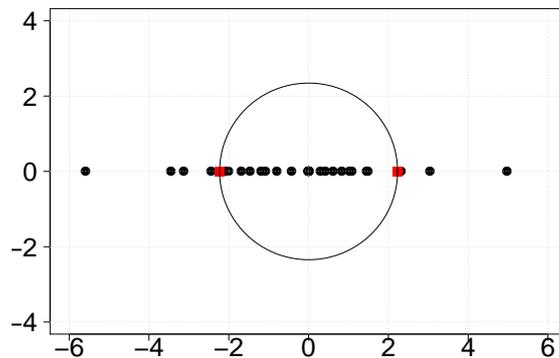
Figure 1: Distribution of the eigenvalues of the Karate network.

3.3. Geometric interpretation

Figure 2 illustrates, for a given bipartition P of the benchmark Karate network, the geometric interpretation of all the vectors of vertices and clusters. This network has 34 vertices. The positive and negative vectors are shown in Figures 2(a) and 2(b), respectively. In these figures, the vectors of clusters are identified by their labels and the solid and dashed lines distinguish the vertex vectors regarding clusters 1 and 2, respectively.

The cluster vectors are the sum of the vertex vectors that compose the clusters. The higher $Rp^{t^T} rp^i$ and the lower $Rn^{t^T} rn^i$, $\forall i \in V$ and $t = \mathcal{C}_P(i)$, the higher the modularity. On the one hand, the obvious choice to maximize the magnitude of the positive cluster vectors in Figure 2(a) is to select the vertices whose positive vertex vectors point to the same direction. On the other hand, to minimize the magnitude of the negative cluster vectors in Figure 2(b), the vertices whose negative vertex vectors point to opposite directions should be selected. By comparing Figures 2(a) and 2(b), it is possible to observe that the magnitude of the positive vectors of the clusters is approximately 4.51 times higher than the magnitude of the negative vectors of the clusters.

11

(a) Positive vertex and cluster vectors   (b) Negative vertex and cluster vectors
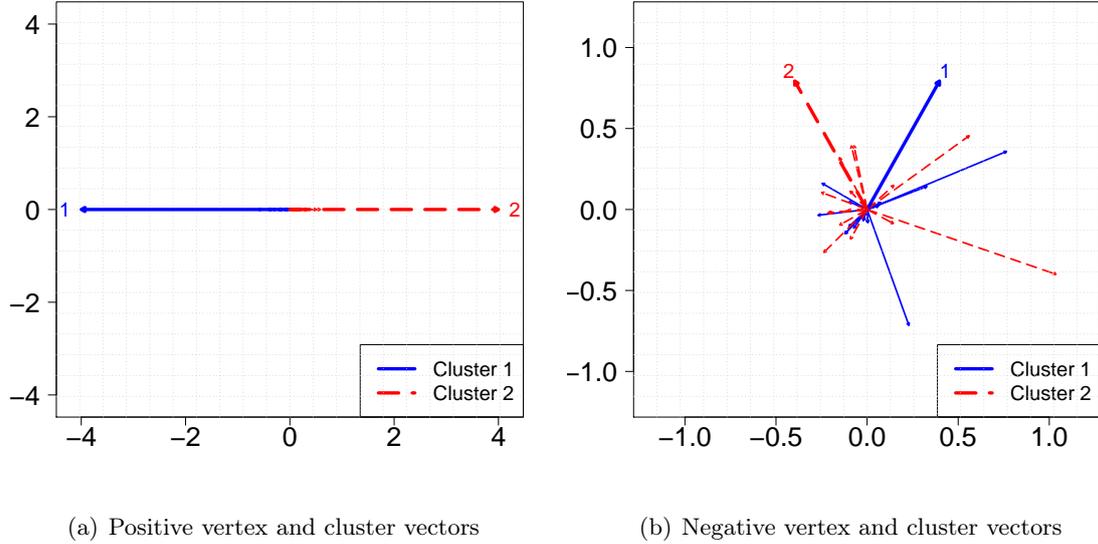
Figure 2: Vectors of the vertices and clusters of the bipartition found by the algorithm proposed in this paper to maximize the weighted aggregate modularity with $\gamma_1 = \gamma_2 = 0.5$ applied to the Karate network.

3.4. Moving vertices between clusters

Given a partition P at hand, some procedures attempt to enhance its quality, which can be evaluated using a fitness function. One way of performing this task is by moving vertices from one cluster to another so that the modified partition has better quality than the previous one. Many studies that employ this type of strategy can be found in the literature, e.g. (Newman, 2006) and (Zhang & Newman, 2015).

Moving a vertex i from a cluster C_b to a cluster C_t modifies the fitness function value, i.e., the weighted aggregate modularity. Let the vectors of clusters C_b and C_t, disregarding the contribution of vertex i, be defined by $Rp^b = \sum_{v \in C_b, v \neq i} rp^v$, $Rn^b = \sum_{v \in C_b, v \neq i} rn^v$, $Rp^t = \sum_{v \in C_t} rp^v$ and $Rn^t = \sum_{v \in C_t} rn^v$.

On the one hand, before moving i to cluster C_t, the vectors of clusters C_b are given by $Rp'^b = Rp^b + rp^i$ and $Rn'^b = Rn^b + rn^i$, respectively. On the other hand, before any movement, the vectors of cluster C_t are $Rp'^t = Rp^t$ and $Rn'^t = Rn^t$. After moving i from cluster C_b to C_t, the vectors of the clusters are $Rp''^b = Rp^b$, $Rp''^t = Rp^t + rp^i$, $Rn''^b = Rn^b$ and $Rn''^t = Rn^t + rn^i$. Equation (11) presents the change in the weighted aggregate modularity of partition P after moving a vertex i from a cluster C_b to a cluster

C_t.

$$\Delta QW(i, C_b, C_t) = \frac{1}{2m} \left[||Rp''^b||^2 - ||Rn''^b||^2 + ||Rp''^t||^2 - ||Rn''^t||^2 \right.$$
$$\left. - (||Rp'^b||^2 - ||Rn'^b||^2 + ||Rp'^t||^2 - ||Rn'^t||^2) \right] \qquad (11)$$
$$= \frac{1}{m} \left[Rp^{t^T} rp^i - Rn^{t^T} rn^i - Rp^{b^T} rp^i + Rn^{b^T} rn^i \right]$$

From Equation (11), it is possible to see that $\Delta QW(i, b, t) \geq 0$ if $(Rp^{t^T} rp^i - Rn^{t^T} rn^i) \geq (Rp^{b^T} rp^i - Rn^{b^T} rn^i)$.

Recently, Zhang & Newman (2015) presented a spectral greedy heuristic to solve the vector partitioning problem considering only positive eigenvalues. In this heuristic, starting from an initial group of vectors, at each iteration, the algorithm moves a vertex i to the cluster C_{t^*} that results in the largest positive gain in modularity. Concerning both positive and negative eigenvalues, a simple greedy heuristic consists of moving vertex i to the cluster C_{t^*} that results in the largest value for $Rp^{t^{*T}} rp^i - Rn^{t^{*T}} rn^i$. Equation (12) defines the choice of t^*.

$$t^* = \arg \max_{t \in \{1, \dots, k\}} \begin{cases} Rp^{t^T} rp^i - Rn^{t^T} rn^i & \text{, if } \mathcal{C}_P(i) \neq t \\ 0 & \text{, if } \mathcal{C}_P(i) = t \end{cases} \qquad (12)$$

If $t^* = \mathcal{C}_P(i)$, vertex i will remain in its original cluster.

4. Proposed Spectral-evolutionary Hybrid Multi-objective Algorithm

This section thoroughly describes the spectral-evolutionary hybrid multi-objective algorithm proposed in this paper and called *MOSpecG*. *MOSpecG* is an iterative two-phase algorithm. At the first phase, the weighted aggregate modularity matrix is updated and its eigen-decomposition is performed. At the second phase, a memetic algorithm works based on the information of the vertex vectors – discussed in the earlier section. To a better understanding of the method, Algorithm 1 presents a pseudocode of *MOSpecG*.

According to Algorithm 1, *MOSpecG* has as input: an undirected unweighted graph G; the size of the Pareto frontier, $N\mathcal{F}$; the number of generations, $N\mathcal{G}$; the number of solutions in the population, $N\mathcal{P}$; the percentage of solutions from the offspring, $N\mathcal{O}$; the number of eigenvalues and eigenvectors to be computed, p; and the number of iterations of the local search procedure, IT.

In line 1 of Algorithm 1, set $\mathcal{F}$ is initialized as empty. Consider that the possible values of γ_1 and γ_2 are defined in a grid to ensure a good spreading of the solutions in the Pareto frontier approximation. Therefore, the grid spacing is dependent on the number of solutions

---

Algorithm 1: *MOSpecG*

    Input   : G, $N\mathcal{F}$, $N\mathcal{G}$, $N\mathcal{P}$, $N\mathcal{O}$, p and IT
    Output: $\mathcal{F}$

1 $\mathcal{F} = \emptyset$
2 $inc = \frac{1}{N\mathcal{F}-1}$
3 for $\gamma_1 = 0$ *to* 1, $\gamma_1 = \gamma_1 + inc$ **do**
4 $\gamma_2 = 1 - \gamma_1$
5   Construct the weighted aggregate modularity matrix BW with weights γ_1 and γ_2
6 $\Lambda, U :=$ Eigen-decomposition of BW regarding the p largest eigenvalues in absolute value
7 $\chi := \max_{\Lambda_{ii}, \forall i}(\Lambda_{ii})$
8 $k' :=$ number of eigenvalues of BW with value larger than or equal to $\sqrt{\chi}$
9 $k := \lfloor 1.25k' \rceil$
10   Define vertex vectors rp^i and rn^i, $\forall i \in V$
11 $P:=$*Memetic Algorithm*($N\mathcal{G}, \mathcal{N}P, \mathcal{N}O, IT, k, rp^i, rn^i, \forall i \in V$)
12 $\mathcal{F} := \mathcal{F} \cup P$
13 end

---

of the resulting Pareto frontier. In line 2, the grid spacing is assigned to variable inc in order to define values for γ_1. In the sequence, weight γ_2 is calculated taking γ_1 as reference, in line 4. From lines 5 to 11, the proposed heuristic creates a new solution to the approximation of the Pareto frontier by optimizing QW with the current values of γ_1 and γ_2.

In particular, in line 5, the algorithm constructs matrix BW with weights γ_1 and γ_2 according to Equation (5). In line 6, the largest p eigenvalues and the associated eigenvectors that compose Λ and U are computed using the *implicitly restarted Arnoldi method* from ARPACK++ library (Lehoucq et al., 1998). In line 7, the leading eigenvalue is assigned to χ. In lines 8 and 9, *MOSpecG* estimates the number of clusters, k, according to Section 3.2. In line 10, vertex vectors rp^i and rn^i, $\forall i \in V$, are defined according to Equations (8) and (9), respectively. In line 11, *MOSpecG* calls the *Memetic Algorithm* function presented in Algorithm 2 to optimize QW with weights γ_1 and γ_2. The resulting partition P is included in the Pareto frontier approximation $\mathcal{F}$ in line 12. At the end, Algorithm 1 returns $\mathcal{F}$.

In the next section, the *Memetic Algorithm* employed in line 11 of Algorithm 1 is comprehensively discussed.

4.1. Memetic Algorithm

Before going into detail on the algorithm, let us briefly introduce the notations employed in this section.

Let the population of the g-ith generation be defined by $\mathcal{P}^g = \{P_1^g, P_2^g, \ldots, P_{N\mathcal{P}}^g\}$, where $g \in \{1, 2, \ldots, N\mathcal{G}\}$. The individuals from the population of the g-ith generation are the partitions P_h^g, $h \in \{1, 2, \ldots, N\mathcal{P}\}$.

Algorithm 2 presents the proposed *Memetic Algorithm*, whose inputs are: $N\mathcal{G}$; $\mathcal{N}P$; $\mathcal{N}O$; IT; the number of clusters, k; and the vertex vectors rp^i and rn^i, $\forall i \in V$. In line 1 of Algorithm 2, the initial population, i.e., individuals from the first generation, is constructed using the strategy suggested by Zhang & Newman (2015). This strategy selects k vertices and assigns each of them to a different cluster (k singletons). Then, the vectors of the selected clusters Rp^t and $Rn^t, t = 1, \ldots, k$, are updated. The remaining vertices are assigned to clusters C_{t^*}, where t^* is chosen according to Equation (12).

Algorithm 2: *Memetic Algorithm*

Input : $N\mathcal{G}$, $N\mathcal{P}$, $N\mathcal{O}$, IT, k, rp^i and rn^i, $\forall i \in V$
Output: Fittest individual P^*

1   $P^1_s, s = 1, \ldots, N\mathcal{P} :=$ construct solution using vertex vectors as directions
2   **for** $g = 1$ *to* $N\mathcal{G}$ **do**
3      $\mathcal{O} := Crossover(\mathcal{P}^g, k, rp^i, rn^i, \forall i \in V)$
4      $\mathcal{O} := Mutation(\mathcal{O}, k, rp^i, rn^i, \forall i \in V)$
5      $\mathcal{O} := LocalSearch(\mathcal{O}, IT, k, rp^i, rn^i, \forall i \in V)$
6      $\mathcal{P}^{g+1} :=$ Update population $\mathcal{P}^g$ using $\mathcal{O}$
7   **end**
8   $P^* :=$ the fittest individual from $\mathcal{P}^{N\mathcal{G}}$

Figure 3 shows an example of an initial partition of the Karate network. To calculate QW, we considered $\gamma_1 = \gamma_2 = 0.5$. In this figure, each square identifies the cluster label of a vertex of the network.

P^1_s | 1 | 2 | 1 | 1 | 1 | 1 | 1 | 1 | 1 | 1 | 1 | 1 | 1 | 1 | 1 | 2 | 2 | 1 | 1 | 2 | 1 | 2 | 1 | 2 | 2 | 2 | 2 | 2 | 2 | 2 | 2 | 2 | 2 | 2 |

$QW(P^1_s) = 0.1443$

Figure 3: Example of a solution for the Karate network when $\gamma_1 = \gamma_2 = 0.5$.

In line 3, the *Memetic Algorithm* constructs the offspring of generation g, $\mathcal{O}$, by applying the genetic operator crossover (Algorithm 3) to the current population $\mathcal{P}^g$. In lines 4 and 5, the genetic operator mutation (Algorithm 4) and a local search procedure (Algorithm 5) update the offspring population. The population of the next generation, $\mathcal{P}^{g+1}$, is the population $\mathcal{P}^g$ but with the $N\mathcal{O}\%$ fittest individuals from the offspring $\mathcal{O}$ replacing the $N\mathcal{O}\%$ least fit individuals from $\mathcal{P}^g$. In line 8, the algorithm returns the fittest individual from $\mathcal{P}^{N\mathcal{G}}$, i.e., individual P^* such that $P^* = \arg\max_{P \in \mathcal{P}^{N\mathcal{G}}} QW(P)$.

4.1.1. Crossover

Algorithm 3 presents the one-way crossover procedure of the *Memetic Algorithm*, which has as input $\mathcal{P}^g$, k, rp^i and rn^i, $\forall i \in V$. At each iteration f, the crossover constructs a

new solution for the offspring population, $\mathcal{O}$, by combining two solutions from the current population $\mathcal{P}^g$. In line 2, the fitness proportionate roulette method selects two individuals P_b^g and P_d^g, $b, d \in \{1, 2, \ldots, N\mathcal{P}\}, b \neq d$, to perform the crossover. In line 3, the algorithm creates an offspring individual W as a copy of P_d^g. In line 4, the method randomly selects a vertex vs and, in line 5, ls stores the label of the cluster of vs in individual P_b^g.

Algorithm 3: *Crossover*

Input : $\mathcal{P}^g$, k, rp^i and rn^i, $\forall i \in V$
Output: $\mathcal{O} = \{O_1, O_2, \ldots, O_{N\mathcal{P}}\}$

1 **for** $f = 1$ *to* $N\mathcal{P}$ **do**
2   Pick randomly P_b^g and P_d^g, $b, d \in \{1, 2, \ldots, N\mathcal{P}\}, b \neq d$, from $\mathcal{P}^g$ with probability
      distribution $pr(P_h^g) = \frac{QW(P_h^g)}{\sum_{P_j^g \in \mathcal{P}} QW(P_j^g)}, h \in \{1, 2, \ldots, N\mathcal{P}\}$.
3     $W := P_d^g$
4   Randomly select a vertex vs from V
5     $ls := P_b^g(vs)$
6     $ld^* :=$ choose according to Equation (13)
7   Move vd to cluster C_{ld^*} in individual W, $\forall vd \in V$ such that $\mathcal{C}_{P_b^g}(vd) = ls$ and
      $\mathcal{C}_W(vd) \neq ld^*$
8   Update QW and cluster vectors
9     $\mathcal{O}f := W$
10 **end**

In line 6, the crossover procedure selects the cluster with label ld^* from individual P_d^g as the cluster whose sum of the inner products $Rp_{ls}^{b\,T} Rp_{ld}^d$ and $Rn_{ls}^{b\,T} Rn_{ld}^d$ is the maximum amongst all $ld \in \{1, \ldots, k\}$, according to Equation (13).

$$ld^* = \arg\max_{ld \in \{1, \ldots, k\}} (Rp_{ls}^{b\,T} Rp_{ld}^d + Rn_{ls}^{b\,T} Rn_{ld}^d) \tag{13}$$

Figure 4 shows an example of the selection performed in line 6 of Algorithm 3. It illustrates the cluster vector with label $ls = 2$ in individual P_b^g, as a solid red line, and the cluster vectors with labels $ld \in \{1, 2\}$ in individual P_d^g – candidates to ld^* – as dashed lines. The positive and negative vectors are identified by the label of the clusters and are shown in Figures 4(a) and 4(b), respectively. The conjecture that justifies the selection choice is that the clusters whose vectors point to the same direction have more vertices in common. In this example, the cluster with label $ld^* = 1$ from individual P_d^g is selected because $Rp_{ls=2}^{b\,T} Rp_{ld^*=1}^d + Rn_{ls=2}^{b\,T} Rn_{ld^*=1}^d$ is higher than $Rp_{ls=2}^{b\,T} Rp_{ld=2}^d + Rn_{ls=2}^{b\,T} Rn_{ld=2}^d$ in individual P_b^g.

In line 7, the method moves the vertices vd in the cluster labeled ls in individual P_b^g to cluster labeled ld^* in individual W. For all $vd \in V$ already belong to the cluster labeled

(a) Positive cluster vectors   (b) Negative cluster vectors
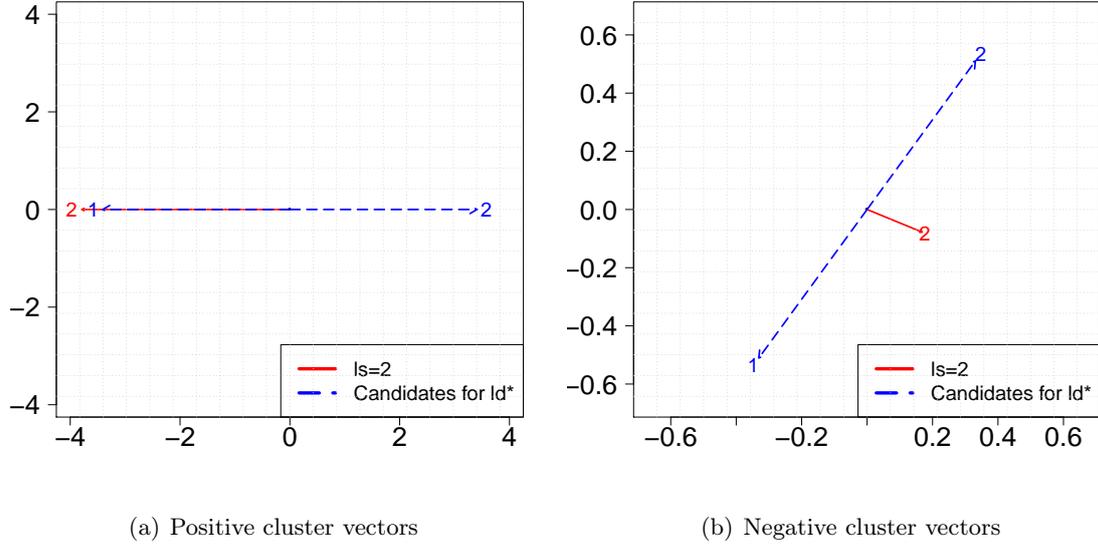
Figure 4: Example of the selection of ld^* performed by the crossover procedure in the Karate network.

ld^*, nothing is done. After each movement, line 8 of Algorithm 3 updates: (i) the weighted aggregate modularity QW, according to Equation (11), and (ii) the vectors of the clusters involved in the vertex moves in individual W, according to Section 3.4. After setting W as the offspring individual $\mathcal{O}_f$ in line 9, the crossover returns the offspring population $\mathcal{O} = \{\mathcal{O}_1, \mathcal{O}_2, \dots, \mathcal{O}_{NP}\}$.

Figure 5 gives an example of the crossover procedure when $\gamma_1 = \gamma_2 = 0.5$. In the example, the offspring individual W had a higher weighted aggregate modularity value than the parents P_b^1 and P_d^1. Let $ls = 2$; the selection of $ld^* = 1$ was illustrated in Figure 4. The vertices whose cluster label is $ls = 2$ on individual P_b^1 are in bold on the partitions. At the offspring individual, which is initially a copy of P_d^1, these vertices are moved to the group labeled $ld^* = 1$, if they are not yet in this group.

4.1.2. Mutation

Algorithm 4 presents the mutation procedure whose inputs are: the offspring population, $\mathcal{O}$; k; rp^i and rn^i, $\forall i \in V$. In line 1, a random integer number in the interval $[1, \lfloor \frac{n}{2} \rfloor]$ is assigned to *count*, which indicates the number of mutations. In line 2, an individual O_d is randomly selected from $\mathcal{O}$. In line 3, the algorithm picks *count* vertices from V at random to define the set of vertices to be mutated, V'. Each vertex $vd \in V'$ is assigned to a cluster C_r chosen randomly from individual O_d, in lines 5 and 6. Note that if a cluster C_t is empty, vd will be assigned to a new cluster. After each movement of a vertex vd, both QW and the vectors of cluster C_r are updated in line 8. The mutation procedure halts when all vertices

P_b^1 `1 2 1 2 2 2 2 2 1 1 2 2 2 2 1 1 2 2 1 2 1 2 1 1 1 1 1 1 1 1 1 1 1 1`

$QW(P_b^1) = 0.1835$

P_d^1 `1 2 1 1 1 1 1 1 1 1 1 1 1 1 1 2 2 1 1 2 1 2 1 2 2 2 2 2 2 2 2 2 2 2`

$QW(P_d^1) = 0.1443$

$ls = $ `2` $ld^* = $ `1`

W `1 1 1 1 1 1 1 1 1 1 1 1 1 1 1 2 2 1 1 2 1 2 1 2 2 2 2 2 2 2 2 2 2 2`

$QW(W) = 0.1868$

Figure 5: Example of the crossover procedure in a partition of the Karate network for $\gamma_1 = \gamma_2 = 0.5$.

of V' have been mutated and, then, returns the updated offspring $\mathcal{O}$.

Algorithm 4: *Mutation*

Input : $\mathcal{O}$, k, rp^i and rn^i, $\forall i \in V$

Output: Updated $\mathcal{O}$

1 Randomly choose an integer number *count* from interval $[1, \lfloor \frac{n}{2} \rfloor]$ with uniform probability distribution

2 Randomly select an individual $\mathcal{O}_d$ from $\mathcal{O}$

3 Randomly pick *count* distinct elements from V and assign them to V'

4 **while** $V' \neq \emptyset$ **do**

5 $\quad$ Randomly choose C_r from the k possible clusters of $\mathcal{O}_d$

6 $\quad$ Move a $vd \in V'$ to cluster C_r, if $\mathcal{C}_{\mathcal{O}_d}(vd) \neq r$

7 $\quad$ $V' := V' \backslash \{vd\}$

8 $\quad$ Update QW and vectors of cluster C_r

9 **end**

Figure 6 presents an example of the mutation procedure on an individual O_d generated to decode a solution for the Karate network. The mutated individual O_d is a result of the modification of the labels of 6 randomly selected vertices.

4.1.3. Local search

Algorithm 5 shows the local search procedure of the introduced *Memetic Algorithm*, which has as input $\mathcal{O}$, IT, k, rp^i and rn^i, $\forall i \in V$. Each iteration of the local search attempts to improve the modularity value of individuals of offspring $\mathcal{O}$ by moving vertices to different communities. In line 4, for each individual $O_d \in \mathcal{O}$ and each vertex $vi \in V$, the local search selects the label t^* such that the relocation of vi to cluster C_{t^*} will result in the largest modularity gain. In line 5, vi is assigned to cluster C_{t^*}, if it does not belong

O_d | 1 | **2** | 2 | 2 | 2 | 2 | 2 | 2 | **2** | 2 | 2 | 2 | **2** | 2 | 1 | 1 | 2 | 2 | 1 | 2 | 1 | 2 | **1** | 1 | 1 | 1 | **1** | 1 | 1 | 2 | **2** | 1 | 1 | 1

$$QW(O_d) = 0.1408$$

Mutated O_d | 2 | **1** | 2 | 2 | 2 | 2 | 2 | 2 | **1** | 2 | 2 | 2 | **1** | 2 | 1 | 1 | 2 | 2 | 1 | 2 | 1 | 2 | **2** | 1 | 1 | 1 | **2** | 1 | 1 | 2 | **1** | 1 | 1 | 1

$$QW(O_d) = 0.0799$$

Figure 6: Example of the mutation procedure on an individual that decodes a solution for the Karate network when $\gamma_1 = \gamma_2 = 0.5$.

to it yet. After moving vi, in line 6 of the algorithm, QW, the vectors of cluster C_{t^*} and the vector of the cluster where vi was found before being moved are updated. Algorithm 5 returns the improved offspring $\mathcal{O}$.

Algorithm 5: Local Search

Input : $\mathcal{O}$, IT, k, rp^i and rn^i, $\forall i \in V$
Output: $\mathcal{O}$

1 **for** $it = 1$ *to* IT **do**
2   **for** $O_d \in \mathcal{O}$ **do**
3   **for** $vi \in V$ **do**
4   Select t^* according to Equation (12)
5   Move vi to cluster C_{t^*} if $\mathcal{C}_{O_d}(vi) \neq t^*$
6   Update QW and the vectors of cluster C_{t^*}
7   **end**
8   **end**
9 **end**
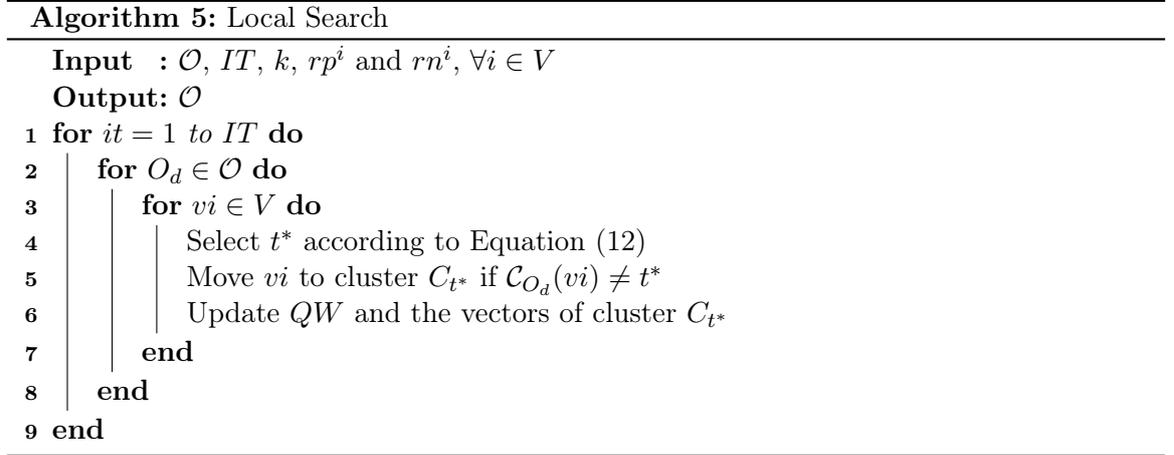
Figure 7 illustrates the local search procedure on an individual of the offspring. In this figure, the procedure improved the weighted aggregate modularity of an individual O_d by moving a single vertex to a different cluster.

O_d | 0 | 1 | **2** | 1 | 1 | 1 | 1 | 1 | 2 | 2 | 1 | 1 | 1 | 1 | 2 | 2 | 1 | 1 | 2 | 1 | 2 | 1 | 2 | 2 | 2 | 2 | 2 | 2 | 2 | 2 | 2 | 2 | 2 | 2

$$QW(O_d) = 0.1835$$

Improved O_d | 1 | 1 | **1** | 1 | 1 | 1 | 1 | 1 | 2 | 2 | 1 | 1 | 1 | 1 | 2 | 2 | 1 | 1 | 2 | 1 | 2 | 1 | 2 | 2 | 2 | 2 | 2 | 2 | 2 | 2 | 2 | 2 | 2 | 2

$$QW(O_d) = 0.1946$$
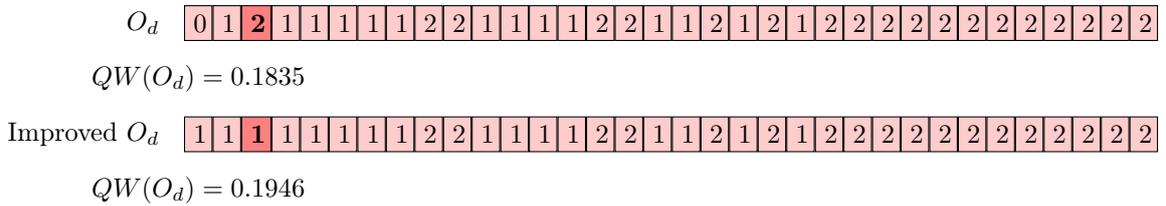
Figure 7: Example of the local search applied to a solution for the Karate network when $\gamma_1 = \gamma_2 = 0.5$.

4.2. Ensemble algorithm

This section introduces an ensemble algorithm that uses information of partitions obtained by *MOSpecG* to find a single partition that best captures the community structure of a network. Algorithm 6 presents the proposed ensemble algorithm, called *SpecG-EC*. The algorithm has as input G; $N\mathcal{G}$; $N\mathcal{P}$; $N\mathcal{O}$; p; IT; a set of partitions, $\mathcal{F}$, and a required threshold, τ. A partition from $\mathcal{F}$ is identified by $\mathcal{F}_i, i = \{1, \ldots, N\mathcal{F}\}$, and represents the solution achieved by *MOSpecG* for $\gamma_1 = (i-1)\frac{1}{N\mathcal{F}-1}, \gamma_2 = 1 - \gamma_1$.

Algorithm 6: *SpecG-EC*

   Input : G, $N\mathcal{G}$, $N\mathcal{P}$, $N\mathcal{O}$, p, IT, $\mathcal{F}$ and τ
   Output: Ensemble partition EP
1 $\mathcal{F}' := \mathcal{F}\backslash\{\mathcal{F}_1, \mathcal{F}_{N\mathcal{F}}\}$
2 $e_{ij} :=$ number of times that $\mathcal{F}'_a(i) = \mathcal{F}'_b(j), \forall \mathcal{F}'_a, \mathcal{F}'_b \in \mathcal{F}', \forall i, j \in V$
3 $\mathcal{E} := \frac{\mathcal{E}}{|\mathcal{F}'|}$
4 $e_{ij} = 0$, if $e_{ij} < \tau, \forall i, j \in V$
5 $A := A + \mathcal{E}$
6 $\Lambda\mathcal{E}, U\mathcal{E} :=$ Eigen-decomposition of B regarding the p largest eigenvalues in absolute value
7 $\chi := \max_{\Lambda\mathcal{E}_{ii}, \forall i}(\Lambda\mathcal{E}_{ii})$
8 $k' :=$ number of eigenvalues of B with values larger than or equal to $\sqrt{\chi}$
9 $k := \lfloor 1.25k' \rfloor$
10 Define vertex vectors rp^i and rn^i, $i \in V$
11 $EP := Memetic\ Algorithm(N\mathcal{G}, N\mathcal{P}, N\mathcal{O}, IT, k, rp^i, rn^i, \forall i \in V)$

Line 1 of Algorithm 6 assigns to $\mathcal{F}'$ every solution from $\mathcal{F}$ except those by *MOSpecG* for the pair of values $\gamma_1 = 0, \gamma_2 = 1$ and $\gamma_1 = 1, \gamma_2 = 0$, i.e., $\mathcal{F}_1$ and $\mathcal{F}_{N\mathcal{F}}$. Let $\mathcal{E} = [e_{ij}] \in \mathbb{R}^{n \times n}$ be a consensus matrix. In lines 2 to 4, $\mathcal{E}$ is defined according to Lancichinetti & Fortunato (2012): in line 2, e_{ij} receives the number of times that vertices i and j appear in the same cluster in the partitions from $\mathcal{F}'$; in line 3, matrix $\mathcal{E}$ is normalized; and, in line 4, elements from $\mathcal{E}$ below a threshold τ are set to 0 to avoid noisy data. In particular, the step described in line 4 is skipped for $i', j' \in V$, where $j' = \arg\max_j e_{i'j}$ and $e_{i'j'} < \tau$.

In order to favor the grouping of vertices that are in the same cluster in the majority of the partitions from $\mathcal{F}'$, in line 5, the ensemble algorithm adjusts the original graph by adding the consensus matrix to the adjacency matrix.

The ensemble algorithm calculates the eigenvalues and eigenvectors of the original modularity matrix B, in line 6. It estimates the number of clusters, k, in lines 7 to 9, according to Section 3.2. In line 10, the vertex vectors rp^i and rn^i, $i \in V$, are created from the eigenvalues and eigenvectors of B. Finally, *SpecG-EC* calls Algorithm 2 to find the partition EP that maximizes the modularity of the adjusted graph in line 11. The ensemble algorithm returns EP.

5. Computational Experiments

This section discusses the computational experiments performed with *MOSpecG* in real and artificial networks. In this section, we refer to *MOSpecG* for maximizing modularity, i.e., with $\gamma_1 = \gamma_2 = 0.5$, as *MOSpecG-mod*. Both *SpecG-EC* and *MOSpecG* were implemented in C++ using the ARPACK++ library[2]. The following values of the parameters were defined in the algorithms after preliminary tests, reported in Appendix A: $N\mathcal{F} = 11$, $\tau = 0.5$, $N\mathcal{G} = 50$, $N\mathcal{P} = 5$, $N\mathcal{O} = 40$ and $p = \lfloor 0.1n \rfloor$. A single parameter was valued differently in experiments with real networks and artificial networks, which is the number of iterations of the local search, IT. In the experiments with real networks, the value of IT was 5, whereas in the experiments with artificial networks, which are much larger than the real networks, IT was valued 1. All the experiments were run on a computer with an Intel Core i7-4790S processor with 3.20GHz and 8GB of main memory.

The experiments are divided into two parts, each of them with two experiments. The first experiment of the first part shows the results obtained by *MOSpecG* with real networks. In this experiment, we present the results including the dominated solutions obtained by *MOSpecG* because some of them had good NMI values. Therefore, we refer to the sets of solutions found by *MOSpecG* as *solution sets* rather than Pareto frontier approximations. In the second experiment of the first part, also with real networks, we contrasted the results achieved by *SpecG-EC* and *MOSpecG-mod* with those found by the reference graph clustering algorithms: Moga-Net, OSLOM and Infomap. Artificial networks were used in the second part of the computational tests. In the first experiment of the second part, we again present the results achieved by *MOSpecG*. In the second experiment, we compared the results achieved by *SpecG-EC* and *MOSpecG-mod* with those obtained by Moga-Net, OSLOM and Infomap. The codes of the reference algorithms used in the experiments are those provided in the authors' website.

In all experiments, the expected partitions of the tested networks are known. Thereby, to evaluate the correlation between the solutions found by the algorithms and the ground truth partitions, we used the measure Normalized Mutual Information (NMI) (Shannon, 1948). The NMI values lie in the range $[0, 1]$ and the higher they are, the more correlated is the pair of partitions.

5.1. Experiments with real networks

This section shows the results of the experiments with the real benchmark networks: Karate (Zachary, 1977), Dolphins (Lusseau et al., 2003), Polbooks (Krebs, 2008) and Foot-

---

[2]The source code is available at `https://github.com/camilapsan/MOSpecG_SpecG`.

ball (Girvan & Newman, 2002). Table 1 presents the number of vertices and edges in these networks.

Table 1: Number of vertices and edges in the real benchmark networks.

	Network			
	Karate	Dolphins	Polbooks	Football
Number of vertices	34	62	105	115
Number of edges	78	159	441	613

5.1.1. Solution sets found by MOSpecG

Figure 8 exhibits the *solution sets* achieved by a single execution of *MOSpecG* for the real benchmark networks. This figure illustrates the trade-offs between the two conflicting objectives. Each point is labeled with the NMI value achieved by the corresponding partitions.

(a) Karate network.

(b) Dolphins network.

(c) Polbooks network.

(d) Football network.
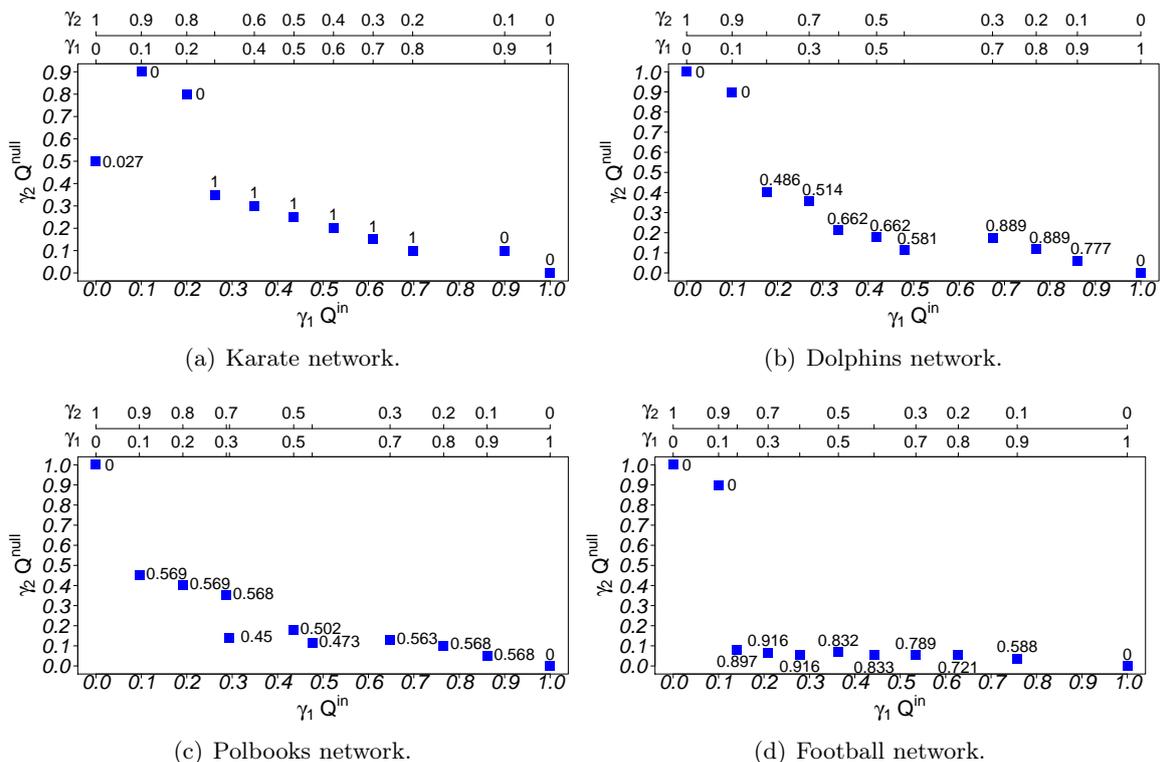
Figure 8: *Solution sets.*

MOSpecG was able to correctly identify the expected partitions of the Karate network for $\gamma_1 \in \{0.3, 0.4, \ldots, 0.8\}$ and $\gamma_2 \in \{0.2, 0.3, \ldots, 0.7\}$. On the one hand, *MOSpecG* achieved the highest NMI values for the Dolphins network when $\gamma_1 Q^{IN} > \gamma_2 Q^{NULL}$ and $\gamma_1 > \gamma_2$. On

the other hand, it achieved the highest NMI values for the Football and Polbooks networks when $\gamma_2 Q^{NULL} > \gamma_1 Q^{IN}$ and $\gamma_2 > \gamma_1$.

Figures 9, 10, 11 and 12 illustrate the partitions found by *SpecG-EC* and *MOSpecG-mod* for the Karate, Dolphins, Polbooks and Football networks, respectively. These figures also report the partitions found by *MOSpecG* with the γ_1 and γ_2 values that resulted in the highest NMI values, here referred to as best partitions. Each vertex is identified by its cluster label in these figures.
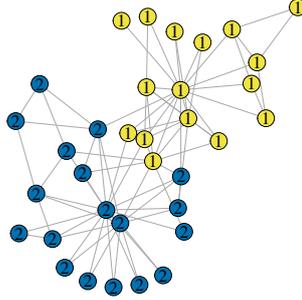
Figure 9: The partition found by *SpecG-EC*, *MOSpecG-mod* and *MOSpecG* with $\gamma_1 \in \{0.3, 0.4, \dots, 0.8\}$ and $\gamma_2 \in \{0.2, 0.3, \dots, 0.7\}$ for the Karate network: NMI value of 1.
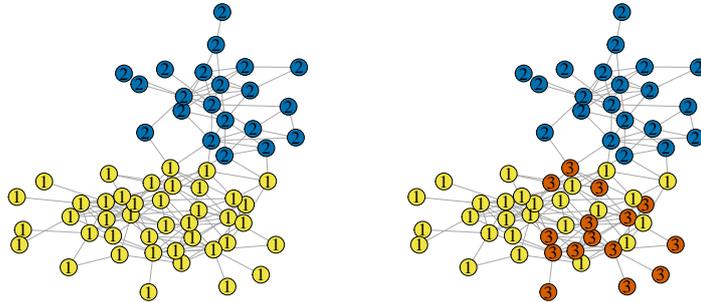
(a) The partition found by *SpecG-EC* and the best partition found by *MOSpecG* with $\gamma_1 \in \{0.7, 0.8\}, \gamma_2 \in \{0.2, 0.3\}$: NMI value of 0.889.

(b) The partition found by *MOSpecG-mod*: NMI value of 0.662.

Figure 10: Dolphins network.

Figure 9 exhibits the expected partition of the Karate network, found by the proposed algorithm. Figure 10 shows that the ensemble and the best partition obtained by *MOSpecG* for the Dolphins network have the expected number of clusters. The cluster with label 3 from the partition returned by *MOSpecG-mod*, in Figure 10(b), is merged with the cluster

23
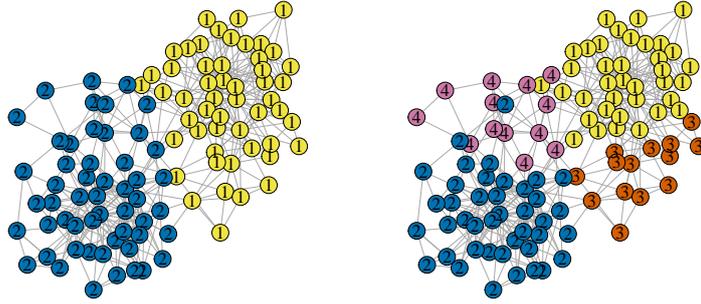
(a) The partition found by *SpecG-EC* and the best partition found by *MOSpecG* with $\gamma_1 \in \{0.1, 0.2\}, \gamma_2 \in \{0.8, 0.9\}$: NMI value of 0.569.

(b) The partition found by *MOSpecG-mod*: NMI value of 0.502.

Figure 11: Polbooks network.
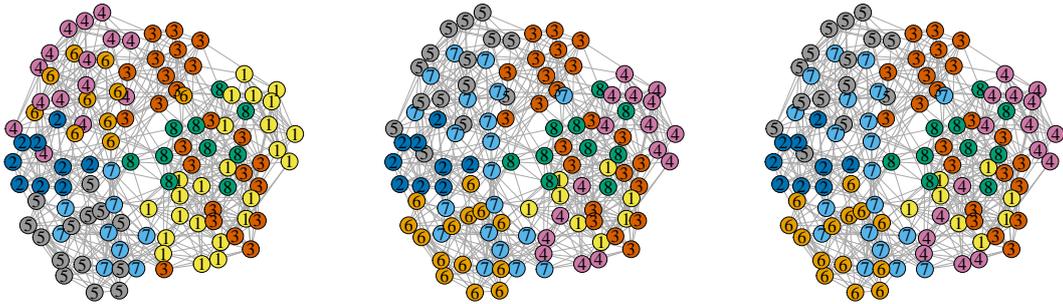
(a) The partition found by *SpecG-EC*: NMI value of 0.839.

(b) The partition found by *MOSpecG-mod*: NMI value of 0.832.

(c) The best partition found by *MOSpecG* with $\gamma_1 = 0.4, \gamma_2 = 0.6$: NMI value of 0.916.

Figure 12: Football network.

with label 1 in the ensemble partition in Figure 10(a). Figure 11 shows that most of the vertices from clusters with labels 3 and 4 in the partition found by *MOSpecG-mod* for the Polbooks network are merged in, respectively, clusters with labels 1 and 2 in the ensemble partition obtained by *SpecG-EC*. None of the partitions found for the Football network in Figure 12 correctly defined the number of clusters.

5.1.2. Comparative analysis

Table 2 reports the average results of ten independent executions of *SpecG-EC*, *MOSpecG-mod*, Moga-Net, OSLOM and Infomap to detect communities in real networks. The results presented are the NMI values, the CPU-times in seconds and number of clusters. The stan-

dard deviation of the presented values is shown between parentheses. Table 2 also presents the number of clusters in the expected partitions.

Table 2: NMI, CPU-times and number of clusters achieved by the algorithms for real graphs.

		Network			
		Karate	Dolphins	Polbooks	Football
SpecG-EC	NMI	**1** (0)	**0.889** (0)	**0.565** (0.006)	0.864 (0.03)
	CPU-time (s)	0.172 (0.05)	0.33 (0.053)	0.884 (0.131)	1.377 (0.203)
	#Clusters	2 (0)	2 (0)	2.3 (0.483)	9 (1.054)
MOSpecG-mod	NMI	**1** (0)	0.662 (0)	0.485 (0.026)	0.876 (0.023)
	CPU-time (s)	0.015 (0.003)	0.025 (0.004)	0.081 (0.015)	0.129 (0.028)
	#Clusters	2 (0)	3 (0)	4.3 (0.483)	9.4 (0.699)
Moga-Net	NMI	0.682 (0.047)	0.538 (0.067)	0.511 (0.054)	0.736 (0.048)
	CPU-time (s)	7.85 (0.627)	11.827 (1.255)	25.231 (2.656)	28.61 (2.888)
	#Clusters	3.9 (0.316)	6.1 (1.449)	5.5 (1.65)	7.8 (1.033)
OSLOM	NMI	**1** (0)	0.786 (0.11)	0.558 (0.017)	0.916 (0)
	CPU-time (s)	0.3 (0.483)	0.9 (0.568)	1.2 (0.422)	0.7 (0.483)
	#Clusters	2 (0)	2 (0)	3.7 (0.675)	11 (0)
Infomap	NMI	0.699 (0)	0.519 (0)	0.537 (0)	**0.924** (0)
	CPU-time (s)	0.2 (0.422)	0.5 (0.527)	0.4 (0.516)	0.4 (0.516)
	#Clusters	3 (0)	6 (0)	5 (0)	12 (0)
Expected	#Clusters	2	2	3	12

As can be seen in Table 2, on the one hand, *SpecG-EC* outperformed Moga-Net in all the networks. On the other hand, *MOSpecG-mod* only found lower NMI values than Moga-Net for the Polbooks network. Moga-Net and Infomap were the only algorithms which did not obtain the expected partition for the Karate network. *SpecG-EC* achieved higher NMI values than all the reference algorithms, including *MOSpecG-mod*, for the Dolphins and Polbooks networks. Furthermore, the number of clusters in the partitions obtained by *SpecG-EC* and *MOSpecG-mod* varied at a maximum of 25% and 43.333%, respectively and on average, when compared to the expected number of clusters. Thereby, there is empirical evidence suggesting the effectiveness of the proposed algorithm in estimating the number of clusters.

The differences between the NMI values reported in Figures 11 and 12 and those presented in Table 2 are due to the fact that the figures only report the results of a single execution, whereas the table shows the average NMI values of ten executions. According to Table 2, the average NMI value of partitions obtained by *SpecG-EC* for the Polbooks network is only 0.703% lower than the highest NMI value of partitions from the *solution set* presented in Figure 8(c). Furthermore, *SpecG-EC* found partitions for Football network whose average NMI value was 5.677% worse than the highest NMI value of partitions from the *solution set* presented in Figure 8(d).

Table 3 demonstrates details of the experiment performed with the proposed and reference algorithms on network Dolphins[3]. The table presents the NMI and modularity values; the running time in seconds; the number of pairs of vertices which were grouped correctly in the same cluster and incorrectly grouped in the same or different clusters, when compared to the expected partition; and the number and size of the clusters in the partitions obtained by the algorithms. The expected partition of network dolphins has 2 clusters with 42 and 20 vertices.

Table 3: Details of the experiment performed using network dolphins.

Algorithm	NMI	Q	CPU-time (s)	Pairs of vertices		Clusters	
				Correct	Wrong	#	Sizes
$MOSpecG$ - $\gamma_1{=}0,\gamma_2{=}1$	0	0	0.018	1051	840	1	62
$MOSpecG$ - $\gamma_1{=}0.1,\gamma_2{=}0.9$	0	0	0.019	1051	840	1	62
$MOSpecG$ - $\gamma_1{=}0.2,\gamma_2{=}0.8$	0.486	0.378	0.025	731	520	2	32, 30
$MOSpecG$ - $\gamma_1{=}0.3,\gamma_2{=}0.7$	0.514	0.391	0.025	754	477	2	33, 29
$MOSpecG$ - $\gamma_1{=}0.4,\gamma_2{=}0.6$	0.662	0.483	0.024	620	451	3	26, 21, 15
$MOSpecG$ - $\gamma_1{=}0.5,\gamma_2{=}0.5$	0.662	0.483	0.022	620	451	3	26, 21, 15
$MOSpecG$ - $\gamma_1{=}0.6,\gamma_2{=}0.4$	0.581	0.518	0.026	492	579	4	21, 20, 14, 7
$MOSpecG$ - $\gamma_1{=}0.7,\gamma_2{=}0.3$	0.889	0.379	0.025	1010	61	2	41, 21
$MOSpecG$ - $\gamma_1{=}0.8,\gamma_2{=}0.2$	0.889	0.379	0.025	1010	61	2	41, 21
$MOSpecG$ - $\gamma_1{=}0.9,\gamma_2{=}0.1$	0.777	0.359	0.025	991	120	2	42, 20
$MOSpecG$ - $\gamma_1{=}1,\gamma_2{=}0$	0	0	0.024	1051	840	1	62
$SpecG$-EC	0.889	0.379	0.281	1010	61	2	41, 21
Moga-Net	0.472	0.417	13.92	532	537	7	31, 10, 6, 6, 4, 3, 2
Infomap	0.519	0.523	1	417	654	6	21, 17, 12, 7, 3, 2
OSLOM	0.814	0.385	1	971	120	2	40, 22

The results in Table 3 show that the larger and the lower the number of pairs of vertices classified correctly and incorrectly, respectively, the larger the NMI values of the partitions. This table also shows that partitions with higher values of modularity are not necessarily more similar to the expected partitions considering the NMI values, the number and size of the clusters. The partition obtained by $SpecG$-EC presented the highest NMI value and matched the expected number of clusters, 2. In this partition, exactly one vertex was classified in the wrong cluster. In combining the solutions of $MOSpecG$ by the consensus strategy, $SpecG$-EC found the partition with the largest NMI. Even though $MOSpecG$ with $\gamma_1 = 0.9$ and $\gamma_2 = 0.1$ and OSLOM identified partitions with 2 clusters and whose numbers of vertices are the expected, 2 vertices were displaced. Both Moga-Net and Infomap identified a large number of clusters, far from the expected.

---

[3]The table additionally reports the results obtained by $MOSpecG$-MO for each combination of γ_1 and γ_2.

5.2. Experiments with artificial networks

This experiment used 80 undirected LFR networks (Lancichinetti et al., 2011) with the following characteristics: 1000 vertices; average degree within the range $[20, 50]$; small-sized communities, whose number of vertices are in the interval $[10, 50]$; large-sized communities, whose number of vertices are in the interval $[20, 100]$; and degree of mixture (mixture coefficient) between groups (μ) with values from the set $\{0.1, 0.2, \ldots, 0.8\}$.

5.2.1. Solution sets found by MOSpecG

Figures 13 to 17 display the average results of the algorithms applied to the LFR networks (y-axis) by μ (x-axis). Figures 13(a) and 13(b) present the average NMI values of partitions obtained by *MOSpecG* for, respectively, the small and large-sized community networks considering each combination of weights γ_1 and γ_2.

(a) Small-sized community networks.

(b) Large-sized community networks.
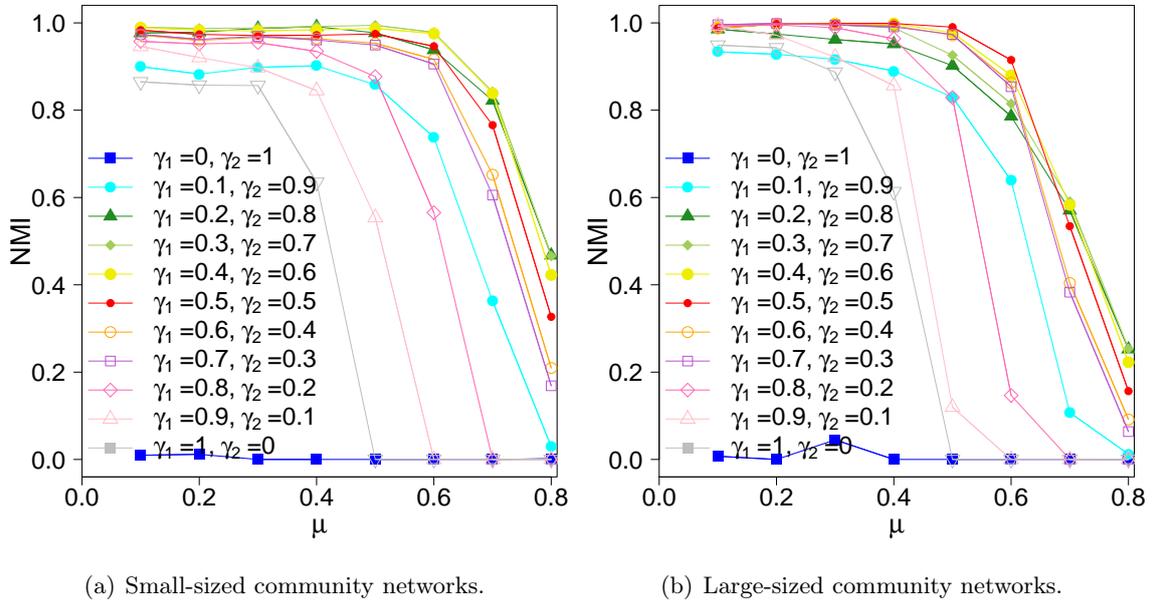
Figure 13: Average NMI values of the partitions obtained by *MOSpecG* considering different values of γ_1 and γ_2.

As can be noted in Figures 13(a) and 13(b), the values of $\gamma_1 \in \{0.2, 0.3\}$ and $\gamma_2 \in \{0.7, 0.8\}$ resulted in partitions with the highest average NMI values for the networks with $\mu \geq 0.7$. The proposed heuristic presented competitive results when detecting communities in all networks by optimizing the modularity, i.e., when $\gamma_1 = \gamma_2 = 0.5$. The partitions found when considering $\gamma_1 = 0$ and $\gamma_2 = 1$ failed to identify good quality clusters.

Figures 14(a) and 14(b) show the average number of clusters in the partitions from the *solution sets* for, respectively, the small and large-sized community networks. Except for the results when $\gamma_1 = 0, \gamma_2 = 1$, which misidentified the number of clusters, and when

$\gamma_1 = 0.1, \gamma_2 = 0.9$, the lower the γ_1 and the larger the γ_2, the larger the number of clusters. Thereby, the number of communities grows with $\gamma = \frac{\gamma_2}{\gamma_1}$.

(a) Small-sized community networks.

(b) Large-sized community networks.
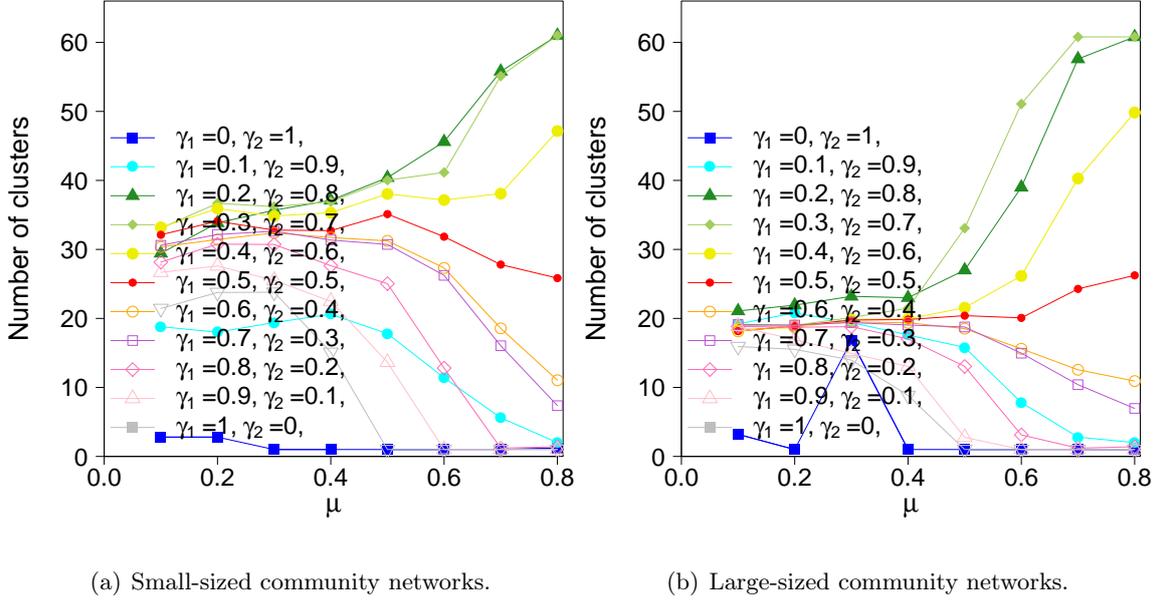
Figure 14: Average number of clusters in the partitions found by *MOSpecG* considering different values of γ_1 and γ_2.

5.2.2. Comparative analysis

Figure 15 presents the average NMI values of the partitions found by *SpecG-EC*, *MOSpecG-mod*, OSLOM, Infomap and Moga-Net whereas Figure 16 shows the respective average CPU-times for the small and large-sized community networks.

Figure 15 shows that the partitions found by *SpecG-EC* and *MOSpecG-mod* had average NMI values higher than those with the largest modularity found by Moga-Net. Moreover, *SpecG-EC* outperformed *MOSpecG-mod*, Infomap and OSLOM in the small-sized community networks with, respectively, $\mu \in \{0.6, 0.7\}$, $\mu \geq 0.7$ and $\mu = 0.8$. In the small-sized community networks with $\mu \leq 0.6$, *SpecG-EC* obtained partitions whose NMI values were higher or equal to 0.953. *SpecG-EC* outperformed *MOSpecG-mod*, Infomap and OSLOM in large-sized community networks with, respectively, $\mu = 0.6$, $\mu \geq 0.6$ and $\mu \in \{0.6, 0.7\}$, and achieved NMI values of at least 0.979 in the networks when $\mu \leq 0.5$.

MOSpecG-mod and Infomap were the algorithms with the lowest CPU-times in networks with, respectively, small and large-sized community networks. Nonetheless, *SpecG-EC* was from 6 to 64 times faster than Moga-Net in all the networks. On the one hand, *SpecG-EC* was faster than OSLOM in the large-sized community networks with $\mu \geq 0.6$. On the other, it required from 1.18 to 3.056 times more than the CPU time required by OSLOM in the
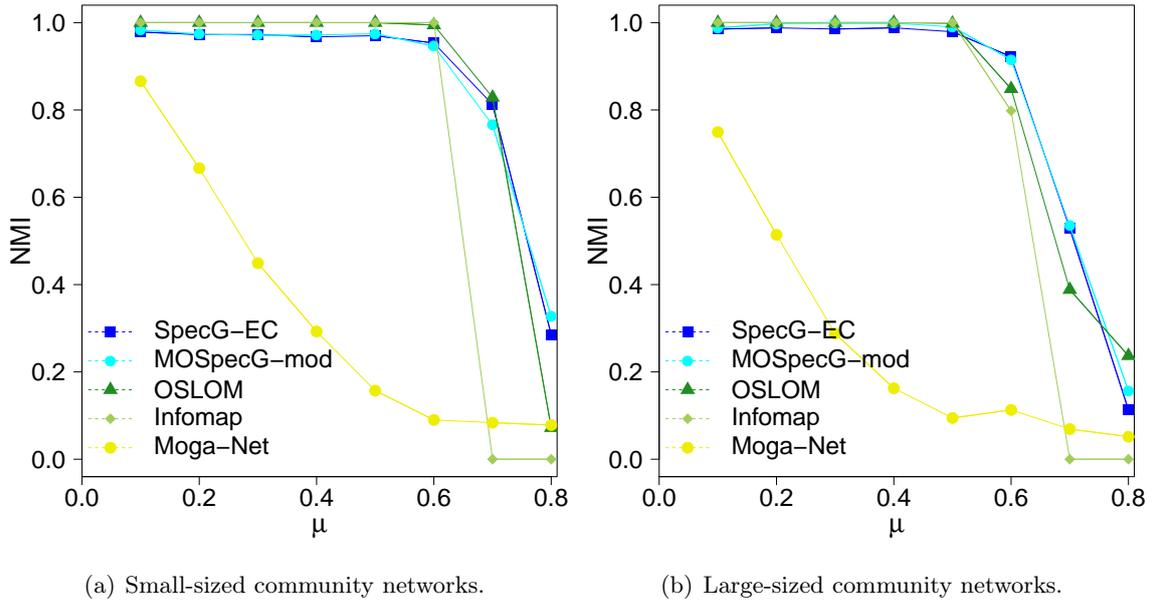
Figure 15: Average NMI values achieved by the algorithms.

(a) Small-sized community networks.   (b) Large-sized community networks.
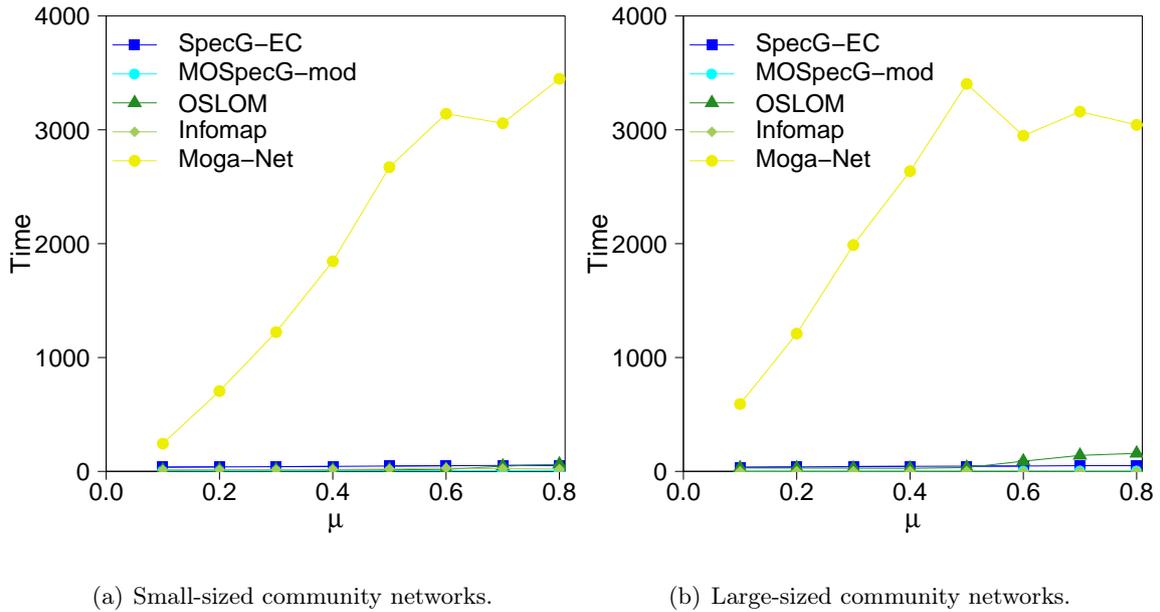
Figure 16: Average CPU-times (s) required by the algorithms.

remaining networks. Because *MOSpecG-mod* was approximately 13.286 times faster than *SpecG-EC*, it was also faster than OSLOM in all the networks.

Figure 17 shows the number of clusters obtained by the algorithms in the partitions and in the expected partitions. As can be seen in Figure 17, Moga-Net obtained the partitions

with the worst estimation of numbers of clusters with regard to the expected partitions. On the one hand, OSLOM and Infomap found partitions whose number of clusters is exactly the expected in small and large-sized community networks with, respectively, $\mu \leq 0.6$ and $\mu \leq 0.5$. On the other hand, as opposed to *SpecG-EC* and *MOSpecG-mod*, Infomap failed to identify the number of clusters in the networks with $\mu \geq 0.7$. OSLOM obtained partitions with worse estimations of the number of clusters with regard to the expected partitions than both versions of the proposed algorithm for small and large-sized community networks with, respectively, $\mu = 0.8$ and $\mu \geq 0.7$. In particular, despite presenting slightly better NMI values than *SpecG-EC* and *MOSpecG-mod* for large-sized community network with $\mu = 0.8$, OSLOM wrongly identified approximately 381 clusters, on average, more than the expected.

(a) Small-sized community networks.

(b) Large-sized community networks.
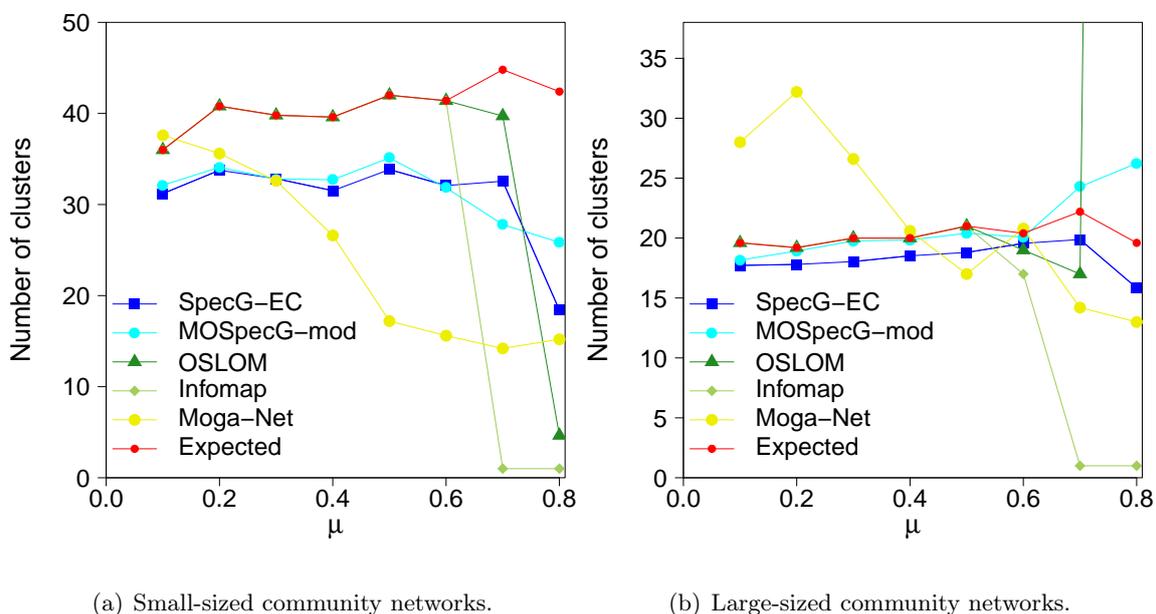
Figure 17: Average number of clusters found by the algorithms in the partitions and in the expected partitions.

6. Final Remarks and Future Works

This paper presented a novel spectral decomposition of modularity to clustering graphs through a multi-objective memetic algorithm called *MOSpecG*. In addition, it introduced an ensemble algorithm, here called *SpecG-EC*, that combines partitions obtained by *MOSpecG* to provide a single partition.

The results of computational experiments using real and LFR networks showed that *SpecG-EC* and the version of *MOSpecG* that maximizes modularity, named *MOSpecG-mod*, outperformed a multi-objective genetic algorithm found in the literature and pre-

sented reasonable running times when compared to reference algorithms. The *SpecG-EC* and *MOSpecG-mod* found partitions more similar to the expected ones than state-of-the-art mono-objective algorithms in artificial networks with higher mixture coefficients and satisfactory results in the remaining artificial networks. In particular, *SpecG-EC* performed better in artificial large-sized community networks and outperformed state-of-the-art mono-objective algorithms in two real networks.

Because *SpecG-EC* obtained better results than *MOSpecG-mod* for most of the networks, we can conclude that the ensemble strategy outperformed the maximization of the classical modularity. Nonetheless, *SpecG-EC* constructs its solution using partitions found by *MOSpecG* and thus is slower than *MOSpecG-mod*. The experiments also suggested that both the ensemble and the modularity maximization version of the proposed algorithm provide a reasonable number of clusters in real and artificial networks.

The empirical finding that some partitions obtained by *MOSpecG* were more similar to the expected partitions than both the modularity maximization and ensemble partitions suggests advantages of studying the duality between the terms of the modularity using multi-objective graph clustering algorithms. In this sense, as future work, we intend to further improve the results achieved by *SpecG-EC* by studying more effective procedures to select partitions from multi-objective problems for the ensemble.

To combine pairs of vertex partitions, evolutionary algorithms usually match the communities of the different partitions to then perform the crossover operator. The matching of the communities is difficult to establish. In *SpecG-EC*, however, we propose a spectral analysis to this step. Unfortunately, *SpecG-EC* does not scale well due to the computational burden in the eigenvalues and eigenvectors computation. Therefore, reducing the computational cost of the spectral decomposition would make this algorithm more effective in detecting communities in larger graphs. As in applications the networks are mostly sparse, a future research direction would be the study of the spectral decomposition of the non-backtracking matrix as the fitness function to reduce the cost of the eigen-decomposition operations of *SpecG-EC*.

Moreover, it is worth to highlight that in many case-oriented applications, such as the study of metabolic networks, the specialist who performs the cluster analysis prefers to investigate the results of a set of solutions instead of a unique partition. In fact, hierarchical clustering algorithms are widely employed in these studies, primarily due to the unclear definition of clustering and the diversified characteristics of the applications. Therefore, in this sense, *MOSpecG* can be a powerful tool, since it provides a pool of solutions from the optimization of the bi-objective problem.

Acknowledgments

References

Amiri, B., Hossain, L., & Crawford, J. (2012). A hybrid evolutionary algorithm based on HSA and cls for multi-objective community detection in complex networks. In *2012 IEEE/ACM International Conference on Advances in Social Networks Analysis and Mining* (pp. 243–247). https://doi.org/10.1109/ASONAM.2012.49.

Amiri, B., Hossain, L., & Crawford, J. W. (2011). An efficient multiobjective evolutionary algorithm for community detection in social networks. In *2011 IEEE Congress of Evolutionary Computation (CEC)* (pp. 2193–2199). https://doi.org/10.1109/CEC.2011.5949886.

Amiri, B., Hossain, L., Crawford, J. W., & Wigand, R. T. (2013). Community detection in complex networks: Multi–objective enhanced firefly algorithm. *Knowledge-Based Systems*, *46*, 1 – 11. https://doi.org/10.1016/j.knosys.2013.01.004.

Angelini, L., Boccaletti, S., Marinazzo, D., Pellicoro, M., & Stramaglia, S. (2007). Identification of network modules by optimization of ratio association. *Chaos: An Interdisciplinary Journal of Nonlinear Science*, *17*, 023114. https://doi.org/10.1063/1.2732162.

Berry, J. W., Hendrickson, B., LaViolette, R. A., & Phillips, C. A. (2011). Tolerating the community detection resolution limit with edge weighting. *Physical Review E*, *83*, 056119. https://doi.org/10.1103/PhysRevE.83.056119.

Brandes, U., Delling, D., Gaertler, M., Gorke, R., Hoefer, M., Nikolosk, Z., & Wagner, D. (2008). On modularity clustering. *IEEE Transactions on Knowledge and Data Engineering*, *20*, 172–188. https://doi.org/10.1109/TKDE.2007.190689.

Carvalho, D. M., Resende, H., & Nascimento, M. C. V. (2014). Modularity maximization adjusted by neural networks. In C. K. Loo, K. S. Yap, K. W. Wong, A. Teoh, & K. Huang (Eds.), *Neural Information Processing* (pp. 287–294). Cham: Springer volume 8834 of *Lecture Notes in Computer Science*. https://doi.org/10.1007/978-3-319-12637-1_36.

Chen, D., Zou, F., Lu, R., Yu, L., Li, Z., & Wang, J. (2016). Multi-objective optimization of community detection using discrete teaching–learning-based optimization with decomposition. *Information Sciences*, *369*, 402 – 418. https://doi.org/10.1016/j.ins.2016.06.025.

Cheng, F., Cui, T., Su, Y., Niu, Y., & Zhang, X. (2018). A local information based multi-objective evolutionary algorithm for community detection in complex networks. *Applied Soft Computing*, *69*, 357 – 367. https://doi.org/10.1016/j.asoc.2018.04.037.

Darst, R. K., Nussinov, Z., & Fortunato, S. (2014). Improving the performance of algorithms to find communities in networks. *Physical Review E*, *89*, 032809. https://doi.org/10.1103/PhysRevE.89.032809.

De Meo, P., Ferrara, E., Fiumara, G., & Provetti, A. (2013). Enhancing community detection using a network weighting strategy. *Information Sciences*, *222*, 648–668. https://doi.org/10.1016/j.ins.2012.08.001.

Deb, K., Pratap, A., Agarwal, S., & Meyarivan, T. (2002). A fast and elitist multiobjective genetic algorithm: NSGA-II. *IEEE Transactions on Evolutionary Computation*, *6*, 182–197. https://doi.org/10.1109/4235.996017.

Ehrgott, M. (2005). Multicriteria optimization. Berlin, Heidelberg: Springer volume 491 of *Lecture Notes in Economics and Mathematical Systems*. https://doi.org/10.1007/3-540-27659-9.

Ferrara, E., Meo, P. D., Catanese, S., & Fiumara, G. (2014). Detecting criminal organizations in mobile phone networks. *Expert Systems with Applications*, *41*, 5733 – 5750. https://doi.org/10.1016/j.eswa.2014.03.024.

Fortunato, S., & Barthélemy, M. (2007). Resolution limit in community detection. *Proceedings of the National Academy of Sciences*, *104*, 36. https://doi.org/10.1073/pnas.0605965104.

Ghaffaripour, Z., Abdollahpouri, A., & Moradi, P. (2016). A multi-objective genetic algorithm for community detection in weighted networks. In *2016 Eighth International Conference on Information and Knowledge Technology (IKT)* (pp. 193–199). https://doi.org/10.1109/IKT.2016.7777766.

Girvan, M., & Newman, M. E. (2002). Community structure in social and biological networks. *Proceedings of the National Academy of Sciences*, *99*, 7821–7826. https://doi.org/10.1073/pnas.122653799.

Golbeck, J., Grimes, J. M., & Rogers, A. (2010). Twitter use by the us congress. *Journal of the Association for Information Science and Technology*, *61*, 1612–1621. https://doi.org/10.1002/asi.21344.

Gong, M., Cai, Q., Chen, X., & Ma, L. (2014). Complex network clustering by multiobjective discrete particle swarm optimization based on decomposition. *IEEE Transactions on Evolutionary Computation*, *18*, 82–97. https://doi.org/10.1109/TEVC.2013.2260862.

Gong, M., Chen, X., Ma, L., Zhang, Q., & Jiao, L. (2013). Identification of multi-resolution network structures with multi-objective immune algorithm. *Applied Soft Computing*, *13*, 1705 – 1717. https://doi.org/10.1016/j.asoc.2013.01.018.

Gong, M., Hou, T., Fu, B., & Jiao, L. (2011). A non-dominated neighbor immune algorithm for community detection in networks. In *Proceedings of the 13th Annual Conference on Genetic and Evolutionary Computation* GECCO '11 (pp. 1627–1634). New York, NY, USA: ACM. https://doi.org/10.1145/2001576.2001796.

Gong, M., Ma, L., Zhang, Q., & Jiao, L. (2012). Community detection in networks by using multiobjective evolutionary algorithm with decomposition. *Physica A: Statistical Mechanics and its Applications*, *391*, 4050–4060. https://doi.org/10.1016/j.physa.2012.03.021.

Kanawati, R. (2015). Empirical evaluation of applying ensemble methods to ego-centred community identification in complex networks. *Neurocomputing*, *150*, 417 – 427. Special Issue on Information Processing and Machine Learning for Applications of Engineering Solving Complex Machine Learning Problems with Ensemble Methods Visual Analytics using Multidimensional Projections. https://doi.org/10.1016/j.neucom.2014.09.042.

Khadivi, A., Rad, A. A., & Hasler, M. (2011). Network community-detection enhancement by proper weighting. *Physical Review E*, *83*, 046104. https://doi.org/10.1103/PhysRevE.83.046104.

Krebs, V. (2008). A network of books about recent us politics sold by the online book-seller amazon.com. URL: `http://www-personal.umich.edu/~mejn/netdata/` Accessed 13 october 2018.

Krzakala, F., Moore, C., Mossel, E., Neeman, J., Sly, A., Zdeborová, L., & Zhang, P. (2013). Spectral redemption in clustering sparse networks. *Proceedings of the National Academy of Sciences*, *110*, 20935–20940. https://doi.org/10.1073/pnas.1312486110.

Lancichinetti, A., Fortunato, S., & Radicchi, F. (2008). Benchmark graphs for testing community detection algorithms. *Physical Review E*, *78*, 046110. https://doi.org/10.1103/PhysRevE.78.046110.

Lancichinetti, A., Radicchi, F., Ramasco, J. J., & Fortunato, S. (2011). Finding statistically significant communities in networks. *PLOS ONE*, *6*, 1–18. https://doi.org/10.1371/journal.pone.0018961.

Lancichinetti, A., & Fortunato, S. (2012). Consensus clustering in complex networks. *Scientific Reports*, *2*, 336. https://doi.org/10.1038/srep00336.

Larsson, A. O., & Moe, H. (2012). Studying political microblogging: Twitter users in the 2010 swedish election campaign. *New Media & Society*, *14*, 729–747. https://doi.org/10.1177/1461444811422894.

Lehoucq, R. B., Sorensen, D. C., & Yang, C. (1998). ARPACK users' guide: solution of large-scale eigenvalue problems with implicitly restarted arnoldi methods. SIAM volume 6 of *Software, Environments, Tools*. https://doi.org/10.1137/1.9780898719628.

Li, Y., Chen, J., Liu, R., & Wu, J. (2012). A spectral clustering-based adaptive hybrid multi-objective harmony search algorithm for community detection. In *2012 IEEE Congress on Evolutionary Computation* (pp. 1–8). IEEE. https://doi.org/10.1109/CEC.2012.6253013.

Liang, Z.-W., Li, J.-P., Yang, F., & Petropulu, A. (2014). Detecting community structure using label propagation with consensus weight in complex network. *Chinese Physics B*, *23*, 098902. https://doi.org/10.1088/1674-1056/23/9/098902.

Lusseau, D., Schneider, K., Boisseau, O., Haase, P., Slooten, E., & Dawson, S. (2003). The bottlenose dolphin community of doubtful sound features a large proportion of long-lasting associations. *Behavioral Ecology and Sociobiology*, *54*, 396–405. https://doi.org/10.1007/s00265-003-0651-y.

Nascimento, M. C. V., de Toledo, F. M. B., & Carvalho, A. C. P. L. F. (2009). Consensus clustering using spectral theory. In M. Köppen, N. Kasabov, & G. Coghill (Eds.), *Advances in Neuro-Information Processing* (pp. 461–468). Berlin, Heidelberg: Springer volume 5506 of *Lecture Notes in Computer Science*. https://doi.org/10.1007/978-3-642-02490-0_57.

Newman, M. E. J., & Girvan, M. (2004). Finding and evaluating community structure in networks. *Physical Review E*, *69*, 026113. https://doi.org/10.1103/PhysRevE.69.026113.

Newman, M. E. J. (2006). Finding community structure in networks using the eigenvectors of matrices. *Physical Review E*, *74*, 036104. https://doi.org/10.1103/PhysRevE.74.036104.

Pizzuti, C. (2008). GA-NET: A genetic algorithm for community detection in social networks. In *International Conference on Parallel Problem Solving from Nature* (pp. 1081–1090). Springer. https://doi.org/10.1007/978-3-540-87700-4_107.

Pizzuti, C. (2009). A multi-objective genetic algorithm for community detection in networks. In *2009 21st IEEE International Conference on Tools with Artificial Intelligence* (pp. 379–386). IEEE. https://doi.org/10.1109/ICTAI.2009.58.

Pizzuti, C. (2012). A multiobjective genetic algorithm to find communities in complex networks. *IEEE Transactions on Evolutionary Computation*, *16*, 418–430. https://doi.org/10.1109/TEVC.2011.2161090.

Pourkazemi, M., & Keyvanpour, M. R. (2017). Community detection in social network by using a multi-objective evolutionary algorithm. *Intelligent Data Analysis*, *21*, 385–409. https://doi.org/10.3233/IDA-150429.

Raghavan, U. N., Albert, R., & Kumara, S. (2007). Near linear time algorithm to detect community structures in large-scale networks. *Physical Review E*, *76*, 036106. https://doi.org/10.1103/PhysRevE.76.036106.

Rahimi, S., Abdollahpouri, A., & Moradi, P. (2018). A multi-objective particle swarm optimization algorithm for community detection in complex networks. *Swarm and Evolutionary Computation*, *39*, 297 – 309. https://doi.org/10.1016/j.swevo.2017.10.009.

Reichardt, J., & Bornholdt, S. (2006). Statistical mechanics of community detection. *Physical Review E*, *74*, 016110. https://doi.org/10.1103/PhysRevE.74.016110.

Rosvall, M., & Bergstrom, C. T. (2008). Maps of random walks on complex networks reveal community structure. *Proceedings of the National Academy of Sciences*, *105*, 1118–1123. https://doi.org/10.1073/pnas.0706851105.

Santos, C. P., Carvalho, D. M., & Nascimento, M. C. (2016). A consensus graph clustering algorithm for directed networks. *Expert Systems with Applications*, *54*, 121–135. https://doi.org/10.1016/j.eswa.2016.01.026.

Shang, R., Luo, S., Zhang, W., Stolkin, R., & Jiao, L. (2016). A multiobjective evolutionary algorithm to find community structures based on affinity propagation. *Physica A: Statistical Mechanics and its Applications*, *453*, 203 – 227. https://doi.org/10.1016/j.physa.2016.02.020.

Shannon, C. E. (1948). A mathematical theory of communication. *Bell System Technical Journal*, *27*, 379–423. https://doi.org/10.1002/j.1538-7305.1948.tb01338.x.

Shi, C., Yan, Z., Cai, Y., & Wu, B. (2012). Multi-objective community detection in complex networks. *Applied Soft Computing*, *12*, 850–859. https://doi.org/10.1016/j.asoc.2011.10.005.

Wei, Y.-C., & Cheng, C.-K. (1991). Ratio cut partitioning for hierarchical designs. *IEEE Transactions on Computer-Aided Design of Integrated Circuits and Systems*, *10*, 911–921. https://doi.org/10.1109/43.87601.

Xu, B., Qi, J., Zhou, C., Hu, X., Xu, B., & Sun, Y. (2015). Hybrid self-adaptive algorithm for community detection in complex networks. *Mathematical Problems in Engineering*, *2015*. https://doi.org/10.1155/2015/273054.

Zachary, W. W. (1977). An information flow model for conflict and fission in small groups. *Journal of Anthropological Research*, *33*, 452–473. https://doi.org/10.1086/jar.33.4.3629752.

Žalik, K. R., & Žalik, B. (2018). Multi-objective evolutionary algorithm using problem-specific genetic operators for community detection in networks. *Neural Computing and Applications*, *30*, 2907–2920. https://doi.org/10.1007/s00521-017-2884-0.

Zhang, X., & Newman, M. (2015). Multiway spectral community detection in networks. *Physical Review E*, *92*, 052808. https://doi.org/10.1103/PhysRevE.92.052808.

Zhou, X., Liu, Y., & Li, B. (2016). A multi-objective discrete cuckoo search algorithm with local search for community detection in complex networks. *Modern Physics Letters B*, *30*, 1650080. https://doi.org/10.1142/S0217984916500809.

Zhu, Z., Wang, C., Ma, L., Pan, Y., & Ding, Z. (2008). Scalable community discovery of large networks. *WAIM '08 Proceedings of the 2008 The Ninth International Conference on Web-Age Information Management*, (pp. 381–388). https://doi.org/10.1109/WAIM.2008.13.

Zou, F., Chen, D., Huang, D.-S., Lu, R., & Wang, X. (2019). Inverse modelling-based multi-objective evolutionary algorithm with decomposition for community detection in complex networks. *Physica A: Statistical Mechanics and its Applications*, *513*, 662 – 674. https://doi.org/10.1016/j.physa.2018.08.077.

Zou, F., Chen, D., Li, S., Lu, R., & Lin, M. (2017). Community detection in complex networks: Multi-objective discrete backtracking search optimization algorithm with decomposition. *Applied Soft Computing*, *53*, 285 – 295. https://doi.org/10.1016/j.asoc.2017.01.005.

Appendix A. Setting up parameters

In this appendix, we present the preliminary experiments carried out using LFR and real networks to fine-tune the parameters of the proposed algorithms. First, we identified the best parameters for *MOSpecG-mod*, which is *MOSpecG* when maximizing the classical version of the modularity measure. After these parameters have been defined, we decide the best value of the parameters $N\mathcal{F}$ and τ of *SpecG-EC*.

Tables A.4, A.5, A.6 and A.7 present the results achieved by *MOSpecG-mod* to detect communities in LFR networks. Tables A.8 and A.9 demonstrate the average results of 10 independent executions of *MOSpecG-mod* to find partitions of the real networks Karate (Zachary, 1977), Dolphins (Lusseau et al., 2003), Polbooks (Krebs, 2008) and Football (Girvan & Newman, 2002). These tables show the NMI values of the partitions with respect to the expected ones and the respective execution times in seconds of *MOSpecG-mod*. All possible combinations of the following parameter values were considered in these experiments: $N\mathcal{G} \in \{10, 50\}$, $N\mathcal{P} \in \{5, 10\}$, $N\mathcal{O} \in \{10, 40, 70\}$, $p \in \{\lfloor 0.1n \rfloor, \lfloor 0.3n \rfloor, \lfloor 0.5n \rfloor\}$ and $IT \in \{1, 5\}$. In addition, Tables A.4, A.5, A.6 and A.7 report the average (AVG), maximum (MAX) and minimum (MIN) NMI values and execution times in detecting communities in the networks with each mixture coefficient value. The shades of gray used as background colors of the table cells are in accordance with the NMI values.

In Tables A.10 and A.11, we show the Pearson correlation coefficients[4] between the *MOSpecG-mod* parameters and (i) the NMI values of the partitions with respect to the expected partitioning of LFR networks considering each possible value of μ, and (ii) the corresponding average (AVG), maximum (MAX) and minimum (MIN) execution times. Table A.12 presents the Pearson correlation coefficients between the *MOSpecG-mod* parameters and the NMI values and execution time in seconds for real networks.

As expected, the parameter p, which refers to the number of eigenvalues and eigenvectors used in the spectral relaxation, presented the highest positive correlation coefficient values with respect to the execution times. On the one hand, the correlation coefficients between p and the NMI values were lower than 0 for small- and large-sized community networks with, respectively, $\mu \leq 0.2$ and $\mu \leq 0.5$. On the other, when considering networks with $\mu \geq 0.7$, the correlation coefficients between p and the NMI values ranged from 0.197 to 0.903. The Pearson correlations between p and the NMI values of the real network partitions were also conflicting: their values were -0.803, 0.406 and 0.374 for Karate, Polbooks and Football networks, respectively. Therefore, in spite of being difficult to draw general conclusions by these results, we remark that the NMI values of partitions of LFR networks increased with p only in networks with high mixture coefficients.

In addition, according to Tables A.10 and A.11, one can also observe that the correlations between $N\mathcal{P}$ and the NMI values of the partitions of LFR networks with $\mu \leq 0.7$ were at least 0.371. Nevertheless, the correlations were -0.109 and -0.226 when considering small- and large-sized community networks with $\mu = 0.8$. One conjecture that might justify the negative correlations in such cases is that *MOSpecG-mod* has more chance of selecting high-

---

[4]The Pearson correlation coefficient assesses the linear correlation between two variables. It is valued from -1 to 1, where -1 and 1 indicate a perfect negative and positive linear correlation, respectively; the value 0 indicates no linear correlation between the pair of variables.

quality partitions more often for the crossover operator when $N\mathcal{P}$ is lower. Tables A.10, A.11 and A.12 also show that regardless the network under consideration the execution time increases alongside $N\mathcal{P}$.

In the parameter-tuning, we selected the set of parameters for *MOSpecG-mod* to obtain partitions with satisfactory NMI values taking a reasonable running time. In line with this, parameters p and $N\mathcal{P}$ received values $\lfloor 0.1n \rfloor$ and 5, respectively. Nonetheless, we recommend setting higher values for p and $N\mathcal{P}$ when the networks under study have high and low mixture coefficients, respectively.

The correlation coefficients between parameter $N\mathcal{O}$ and the NMI values did not present a clear pattern when considering the LFR networks showed in Tables A.10 and A.11. On the one hand, these correlations were at least 0.463 when $\mu \leq 0.7$. On the other, they were -0.157 and -0.286 respectively for small- and large-community size networks with $\mu = 0.8$. Since increasing $N\mathcal{O}$ does not augment the execution times, we adopted the median value to this parameter, 40.

$N\mathcal{G}$ and IT did not have a strong correlation with the NMI values for the LFR networks even though the execution times increased alongside $N\mathcal{G}$ and IT. When considering the real networks, however, the correlations between $N\mathcal{G}$ and the NMI values shown in Table A.12 ranged from 0.034 to 0.211. We therefore considered $N\mathcal{G} = 50$ to enhance the robustness of *MOSpecG-mod*. Because the parameter IT only showed a strong correlation with the NMI value of the partition obtained to the Polbooks network, we used the lowest value of IT, 1, to carry out the experiments with the LFR networks. Nevertheless, in small networks such as the real networks tested in the experiments presented in this paper, we recommend increasing IT since the computational time is significantly low in practice.

Therefore, we chose the following values of parameters: $N\mathcal{G} = 50, N\mathcal{P} = 5, N\mathcal{O} = 40,$ $p = \lfloor 0.1n \rfloor$. The parameter IT was 1 in tests with LFR networks and 5 in the experiments with real networks.

Tables A.13, A.14 and A.15 show the NMI values of the partitions obtained by *SpecG-EC* in small- and large-sized community networks with different mixture coefficients and in real networks. This experiment was performed by fixing the values of $N\mathcal{G}, N\mathcal{P}, N\mathcal{O}$ and p at values decided on the previous parameter tuning experiments and considering the respective combination of the remaining parameters: $N\mathcal{F} \in \{6, 11\}$ and $\tau \in \{0.1, 0.25, 0.5, 0.75\}$. In addition, Tables A.13 and A.14 report the average (AVG), maximum (MAX) and minimum (MIN) values of NMI and execution times in seconds of the consensus step in *SpecG-EC* considering the networks with different mixture coefficients. Even though we did not report the running times of *SpecG-EC* to obtain the $N\mathcal{F}$ partitions required to define the consensus partition, the average execution times increase alongside $N\mathcal{F}$ and τ.

According to Tables A.13 and A.14, the highest NMI values were achieved when $N\mathcal{F} = 11$

and $\tau = 0.75$. Considering Table A.15, the highest NMI values were obtained when $N\mathcal{F} = 11$ and $\tau = 0.5$. The NMI values of partitions of the LFR networks with $\mu \leq 0.5$ when $\tau = 0.5$ were on average only 2% worse than the NMI values of partitions when $\tau = 0.75$. As considering the real networks *SpecG-EC* performed better when τ was fixed at 0.5, we assigned 0.5 to parameter τ.

Table A.4: Experiments to adjust parameters of *MOSpecG-mod* to small-sized community networks - part 1.

Parameters					μ								NMI			Time (s)		
$N\mathcal{G}$	$N\mathcal{P}$	$N\mathcal{O}$	p	IT	0.1	0.2	0.3	0.4	0.5	0.6	0.7	0.8	AVG	MAX	MIN	AVG	MAX	MIN
10	5	10	$\lfloor 0.1n \rfloor$	10	0.901	0.882	0.887	0.907	0.853	0.774	0.55	0.323	0.76	0.907	0.323	3.939	4.563	3.396
10	5	10	$\lfloor 0.1n \rfloor$	50	0.886	0.882	0.897	0.896	0.844	0.769	0.55	0.327	0.756	0.897	0.327	5.86	6.632	5.321
10	5	10	$\lfloor 0.3n \rfloor$	10	0.849	0.838	0.851	0.831	0.781	0.697	0.589	0.469	0.738	0.851	0.469	11.346	13.567	7.686
10	5	10	$\lfloor 0.3n \rfloor$	50	0.841	0.838	0.858	0.83	0.781	0.69	0.597	0.465	0.738	0.858	0.465	28.864	36.643	13.642
10	5	10	$\lfloor 0.5n \rfloor$	10	0.821	0.81	0.822	0.798	0.761	0.685	0.634	0.548	0.735	0.822	0.548	20.778	28.898	12.412
10	5	10	$\lfloor 0.5n \rfloor$	50	0.829	0.811	0.82	0.803	0.758	0.695	0.629	0.542	0.736	0.829	0.542	60.065	91.883	22.256
10	5	40	$\lfloor 0.1n \rfloor$	10	0.985	0.98	0.98	0.969	0.968	0.943	0.767	0.331	0.865	0.985	0.331	1.865	2.118	1.689
10	5	40	$\lfloor 0.1n \rfloor$	50	0.979	0.977	0.979	0.972	0.969	0.952	0.79	0.339	0.87	0.979	0.339	4.136	4.53	3.498
10	5	40	$\lfloor 0.3n \rfloor$	10	0.981	0.98	0.999	0.999	0.996	0.99	0.919	0.409	0.909	0.999	0.409	10.05	13.067	5.876
10	5	40	$\lfloor 0.3n \rfloor$	50	0.98	0.983	0.997	0.999	0.999	0.998	0.937	0.411	0.913	0.999	0.411	29.572	38.344	11.395
10	5	40	$\lfloor 0.5n \rfloor$	10	0.988	0.987	0.998	0.999	1	0.997	0.903	0.469	0.918	1	0.469	20.374	27.569	12.813
10	5	40	$\lfloor 0.5n \rfloor$	50	0.986	0.987	1	1	1	0.999	0.959	0.456	0.923	1	0.456	61.71	100.439	22.056
10	5	70	$\lfloor 0.1n \rfloor$	10	0.981	0.981	0.973	0.969	0.969	0.953	0.749	0.33	0.863	0.981	0.33	2.335	2.622	1.896
10	5	70	$\lfloor 0.1n \rfloor$	50	0.984	0.981	0.98	0.969	0.973	0.953	0.779	0.334	0.869	0.984	0.334	4.728	5.086	3.979
10	5	70	$\lfloor 0.3n \rfloor$	10	0.983	0.98	0.997	1	0.997	0.99	0.916	0.414	0.91	1	0.414	10.37	12.769	6.580
10	5	70	$\lfloor 0.3n \rfloor$	50	0.981	0.983	0.999	1	0.996	0.996	0.942	0.419	0.915	1	0.419	27.99	40.331	11.746
10	5	70	$\lfloor 0.5n \rfloor$	10	0.988	0.99	0.998	0.999	0.999	0.997	0.901	0.464	0.917	0.999	0.464	19.707	26.755	13.802
10	5	70	$\lfloor 0.5n \rfloor$	50	0.983	0.988	0.999	0.999	1	0.999	0.962	0.447	0.922	1	0.447	57.508	92.233	20.299
10	10	10	$\lfloor 0.1n \rfloor$	10	0.987	0.986	0.98	0.973	0.97	0.948	0.749	0.329	0.865	0.987	0.329	2.466	2.823	2.217
10	10	10	$\lfloor 0.1n \rfloor$	50	0.988	0.984	0.982	0.976	0.977	0.958	0.792	0.339	0.875	0.988	0.339	6.916	7.535	5.380
10	10	10	$\lfloor 0.3n \rfloor$	10	0.987	0.985	0.998	0.999	0.996	0.992	0.908	0.418	0.91	0.999	0.418	13.816	17.218	7.192
10	10	10	$\lfloor 0.3n \rfloor$	50	0.985	0.984	0.998	1	1	0.996	0.95	0.419	0.917	1	0.419	49.406	66.762	18.639
10	10	10	$\lfloor 0.5n \rfloor$	10	0.985	0.99	0.999	0.998	0.999	0.997	0.887	0.47	0.916	0.999	0.47	28.757	42.609	13.662
10	10	10	$\lfloor 0.5n \rfloor$	50	0.987	0.99	1	1	1	1	0.947	0.461	0.923	1	0.461	108.069	175.175	36.357
10	10	40	$\lfloor 0.1n \rfloor$	10	0.986	0.98	0.982	0.976	0.973	0.95	0.78	0.331	0.87	0.986	0.331	2.391	2.648	2.184
10	10	40	$\lfloor 0.1n \rfloor$	50	0.989	0.983	0.983	0.982	0.973	0.95	0.793	0.337	0.874	0.989	0.337	7.228	8.476	5.596
10	10	40	$\lfloor 0.3n \rfloor$	10	0.986	0.985	0.999	0.999	1	0.992	0.919	0.411	0.911	1	0.411	14.935	18.538	8.249
10	10	40	$\lfloor 0.3n \rfloor$	50	0.984	0.983	1	0.999	0.999	0.999	0.942	0.411	0.915	1	0.411	49.835	64.276	19.583
10	10	40	$\lfloor 0.5n \rfloor$	10	0.987	0.99	1	0.999	0.999	0.999	0.929	0.482	0.923	1	0.482	28.679	44.118	12.843
10	10	40	$\lfloor 0.5n \rfloor$	50	0.989	0.99	1	1	1	0.999	0.969	0.46	0.926	1	0.46	106.041	175.882	33.539
10	10	70	$\lfloor 0.1n \rfloor$	10	0.992	0.979	0.979	0.976	0.975	0.955	0.754	0.326	0.867	0.992	0.326	2.527	3.088	2.236
10	10	70	$\lfloor 0.1n \rfloor$	50	0.984	0.982	0.982	0.973	0.972	0.956	0.788	0.338	0.872	0.984	0.338	6.912	7.577	5.488
10	10	70	$\lfloor 0.3n \rfloor$	10	0.986	0.981	0.999	0.999	0.998	0.995	0.919	0.411	0.911	0.999	0.411	13.736	17.072	6.914
10	10	70	$\lfloor 0.3n \rfloor$	50	0.985	0.986	0.999	1	0.999	0.997	0.954	0.429	0.919	1	0.429	48.612	64.408	18.673
10	10	70	$\lfloor 0.5n \rfloor$	10	0.99	0.99	0.996	1	0.999	0.998	0.911	0.446	0.916	1	0.446	28.189	42.39	13.094
10	10	70	$\lfloor 0.5n \rfloor$	50	0.986	0.993	0.999	1	1	0.999	0.957	0.453	0.923	1	0.453	106.077	175.132	32.210

Table A.5: Experiments to adjust parameters of *MOSpecG-mod* to small-sized community networks - part 2.

Parameters					μ								NMI			Time (s)		
$N\mathcal{G}$	$N\mathcal{P}$	$N\mathcal{O}$	p	IT	0.1	0.2	0.3	0.4	0.5	0.6	0.7	0.8	AVG	MAX	MIN	AVG	MAX	MIN
50	5	10	⌊0.1n⌋	10	0.899	0.885	0.896	0.892	0.849	0.776	0.542	0.326	0.758	0.899	0.326	4.241	4.554	3.764
50	5	10	⌊0.1n⌋	50	0.885	0.888	0.901	0.892	0.852	0.783	0.562	0.315	0.76	0.901	0.315	15.326	16.689	11.897
50	5	10	⌊0.3n⌋	10	0.849	0.851	0.859	0.819	0.786	0.695	0.595	0.463	0.74	0.859	0.463	26.935	34.837	11.574
50	5	10	⌊0.3n⌋	50	0.851	0.841	0.845	0.823	0.777	0.689	0.597	0.467	0.736	0.851	0.467	114.172	153.981	39.929
50	5	10	⌊0.5n⌋	10	0.826	0.824	0.818	0.795	0.754	0.693	0.633	0.549	0.737	0.826	0.549	57.523	91.836	21.432
50	5	10	⌊0.5n⌋	50	0.824	0.809	0.822	0.792	0.751	0.689	0.633	0.545	0.733	0.824	0.545	250.024	423.033	68.129
50	5	40	⌊0.1n⌋	10	0.984	0.98	0.98	0.971	0.975	0.95	0.779	0.336	0.869	0.984	0.336	4.101	4.582	3.415
50	5	40	⌊0.1n⌋	50	0.986	0.987	0.976	0.977	0.973	0.957	0.812	0.343	0.876	0.987	0.343	15.084	16.476	11.360
50	5	40	⌊0.3n⌋	10	0.979	0.98	0.997	0.999	0.996	0.991	0.909	0.412	0.908	0.999	0.412	27.033	36.392	11.138
50	5	40	⌊0.3n⌋	50	0.985	0.983	0.998	1	0.999	0.996	0.963	0.4	0.916	1	0.4	113.672	152.987	39.445
50	5	40	⌊0.5n⌋	10	0.988	0.99	0.999	0.998	1	0.998	0.928	0.465	0.921	1	0.465	56.769	91.557	20.047
50	5	40	⌊0.5n⌋	50	0.989	0.99	0.999	1	1	1	0.982	0.436	0.925	1	0.436	250.195	421.961	67.939
50	5	70	⌊0.1n⌋	10	0.979	0.978	0.98	0.975	0.967	0.948	0.767	0.336	0.866	0.98	0.336	4.082	4.389	3.398
50	5	70	⌊0.1n⌋	50	0.981	0.975	0.977	0.971	0.968	0.957	0.806	0.342	0.872	0.981	0.342	15.157	16.679	11.699
50	5	70	⌊0.3n⌋	10	0.98	0.981	0.998	0.998	0.996	0.996	0.922	0.413	0.911	0.998	0.413	26.693	34.541	11.423
50	5	70	⌊0.3n⌋	50	0.983	0.983	0.996	0.999	0.998	0.995	0.958	0.425	0.917	0.999	0.425	113.984	152.902	39.230
50	5	70	⌊0.5n⌋	10	0.984	0.982	0.998	0.999	0.997	0.999	0.928	0.478	0.921	0.999	0.478	56.74	91.630	20.113
50	5	70	⌊0.5n⌋	50	0.984	0.986	0.998	1	1	0.999	0.983	0.427	0.922	1	0.427	250.17	421.768	68.330
50	10	10	⌊0.1n⌋	10	0.988	0.98	0.984	0.977	0.974	0.957	0.754	0.332	0.868	0.988	0.332	6.882	7.759	5.594
50	10	10	⌊0.1n⌋	50	0.987	0.982	0.982	0.978	0.978	0.957	0.811	0.344	0.877	0.987	0.344	28.632	31.543	21.711
50	10	10	⌊0.3n⌋	10	0.986	0.985	0.997	0.999	0.997	0.991	0.917	0.416	0.911	0.999	0.416	48.794	64.591	18.255
50	10	10	⌊0.3n⌋	50	0.986	0.987	1	1	0.999	0.998	0.962	0.424	0.92	1	0.424	222.775	300.265	74.748
50	10	10	⌊0.5n⌋	10	0.991	0.989	0.998	1	1	0.996	0.937	0.468	0.922	1	0.468	105.128	174.042	32.190
50	10	10	⌊0.5n⌋	50	0.989	0.989	0.998	1	1	0.999	0.98	0.442	0.925	1	0.442	490.752	833.401	129.655
50	10	40	⌊0.1n⌋	10	0.987	0.983	0.979	0.981	0.973	0.951	0.761	0.332	0.868	0.987	0.332	6.809	7.695	5.380
50	10	40	⌊0.1n⌋	50	0.981	0.983	0.981	0.985	0.972	0.958	0.803	0.346	0.876	0.985	0.346	28.649	31.526	21.613
50	10	40	⌊0.3n⌋	10	0.987	0.981	0.998	1	0.998	0.996	0.937	0.416	0.914	1	0.416	48.478	64.132	18.186
50	10	40	⌊0.3n⌋	50	0.989	0.988	0.998	1	0.999	0.996	0.96	0.41	0.918	1	0.41	222.641	301	74.162
50	10	40	⌊0.5n⌋	10	0.987	0.99	0.998	0.999	0.998	0.998	0.942	0.467	0.922	0.999	0.467	105.672	174.514	32.057
50	10	40	⌊0.5n⌋	50	0.99	0.993	1	1	1	0.999	0.983	0.425	0.924	1	0.425	490.804	834.429	128.175
50	10	70	⌊0.1n⌋	10	0.985	0.985	0.985	0.978	0.977	0.95	0.772	0.33	0.87	0.985	0.33	6.867	7.601	5.289
50	10	70	⌊0.1n⌋	50	0.988	0.984	0.983	0.975	0.972	0.956	0.805	0.341	0.876	0.988	0.341	28.624	31.634	21.670
50	10	70	⌊0.3n⌋	10	0.984	0.984	0.998	0.999	0.998	0.995	0.939	0.418	0.914	0.999	0.418	48.673	64.261	18.514
50	10	70	⌊0.3n⌋	50	0.986	0.985	0.999	1	1	0.998	0.96	0.416	0.918	1	0.416	223.151	300.679	75.510
50	10	70	⌊0.5n⌋	10	0.988	0.99	0.999	1	0.999	0.997	0.953	0.459	0.923	1	0.459	105.182	174.151	31.984
50	10	70	⌊0.5n⌋	50	0.988	0.99	0.998	1	0.999	1	0.983	0.433	0.924	1	0.433	490.98	837.837	128.176

Table A.6: Experiments to adjust parameters of *MOSpecG-mod* to large-sized community networks - part 1.

Parameters					μ								NMI			Time (s)		
$N\mathcal{G}$	$N\mathcal{P}$	$N\mathcal{O}$	p	IT	0.1	0.2	0.3	0.4	0.5	0.6	0.7	0.8	AVG	MAX	MIN	AVG	MAX	MIN
10	5	10	$\lfloor 0.1n \rfloor$	10	0.926	0.931	0.92	0.895	0.795	0.595	0.369	0.188	0.702	0.931	0.188	4.15	4.754	3.774
10	5	10	$\lfloor 0.1n \rfloor$	50	0.927	0.921	0.91	0.886	0.783	0.606	0.354	0.188	0.697	0.927	0.188	5.878	6.711	5.152
10	5	10	$\lfloor 0.3n \rfloor$	10	0.833	0.794	0.748	0.699	0.625	0.507	0.419	0.329	0.619	0.833	0.329	12.368	13.562	10.294
10	5	10	$\lfloor 0.3n \rfloor$	50	0.839	0.789	0.738	0.699	0.624	0.513	0.419	0.327	0.619	0.839	0.327	33.63	38.342	21.380
10	5	10	$\lfloor 0.5n \rfloor$	10	0.803	0.755	0.719	0.662	0.605	0.527	0.484	0.412	0.621	0.803	0.412	23.246	28.721	15.972
10	5	10	$\lfloor 0.5n \rfloor$	50	0.81	0.757	0.719	0.668	0.608	0.528	0.481	0.415	0.623	0.81	0.415	70.536	99.119	35.598
10	5	40	$\lfloor 0.1n \rfloor$	10	1	1	1	1	0.993	0.915	0.537	0.147	0.824	1	0.147	2.629	3.3	2.094
10	5	40	$\lfloor 0.1n \rfloor$	50	1	0.999	0.999	1	0.994	0.923	0.584	0.151	0.831	1	0.151	4.989	5.562	4.291
10	5	40	$\lfloor 0.3n \rfloor$	10	1	1	0.999	1	0.996	0.911	0.524	0.227	0.832	1	0.227	11.791	12.949	9.636
10	5	40	$\lfloor 0.3n \rfloor$	50	1	1	1	1	1	0.965	0.576	0.212	0.844	1	0.212	34.373	38.461	21.337
10	5	40	$\lfloor 0.5n \rfloor$	10	1	1	1	1	0.994	0.879	0.528	0.288	0.836	1	0.288	22.75	28.699	15.740
10	5	40	$\lfloor 0.5n \rfloor$	50	1	1	1	1	1	0.94	0.585	0.273	0.85	1	0.273	71.339	95.149	36.073
10	5	70	$\lfloor 0.1n \rfloor$	10	0.998	1	0.998	0.997	0.991	0.909	0.534	0.156	0.823	1	0.156	2.429	3	2.041
10	5	70	$\lfloor 0.1n \rfloor$	50	1	1	0.999	0.998	0.993	0.92	0.562	0.147	0.827	1	0.147	5.268	6.615	4.113
10	5	70	$\lfloor 0.3n \rfloor$	10	1	1	1	1	0.998	0.926	0.528	0.228	0.835	1	0.228	11.001	11.555	10.506
10	5	70	$\lfloor 0.3n \rfloor$	50	1	1	1	1	1	0.962	0.595	0.213	0.846	1	0.213	31.367	34.998	19.831
10	5	70	$\lfloor 0.5n \rfloor$	10	1	1	0.999	1	0.992	0.875	0.549	0.293	0.839	1	0.293	20.65	26.147	13.595
10	5	70	$\lfloor 0.5n \rfloor$	50	1	1	1	1	0.998	0.957	0.587	0.265	0.851	1	0.265	67.941	93.517	33.107
10	10	10	$\lfloor 0.1n \rfloor$	10	1	1	1	1	0.993	0.917	0.527	0.156	0.824	1	0.156	2.487	2.936	2.125
10	10	10	$\lfloor 0.1n \rfloor$	50	0.999	1	1	1	0.995	0.923	0.558	0.163	0.83	1	0.163	6.855	7.51	6.141
10	10	10	$\lfloor 0.3n \rfloor$	10	1	1	1	1	0.991	0.907	0.516	0.232	0.831	1	0.232	15.943	18.082	10.799
10	10	10	$\lfloor 0.3n \rfloor$	50	1	1	1	1	1	0.952	0.579	0.217	0.844	1	0.217	59.627	73.394	34.367
10	10	10	$\lfloor 0.5n \rfloor$	10	1	1	1	0.995	0.986	0.871	0.523	0.304	0.835	1	0.304	32.498	43.211	18.572
10	10	10	$\lfloor 0.5n \rfloor$	50	1	1	1	1	1	0.936	0.564	0.282	0.848	1	0.282	128.304	179.584	57.375
10	10	40	$\lfloor 0.1n \rfloor$	10	1	1	0.999	1	0.993	0.914	0.546	0.152	0.826	1	0.152	2.584	2.807	2.286
10	10	40	$\lfloor 0.1n \rfloor$	50	1	1	1	1	0.995	0.924	0.557	0.15	0.828	1	0.15	6.831	7.496	6.279
10	10	40	$\lfloor 0.3n \rfloor$	10	1	1	1	1	1	0.924	0.55	0.228	0.838	1	0.228	15.832	17.616	11.098
10	10	40	$\lfloor 0.3n \rfloor$	50	1	1	1	1	1	0.958	0.581	0.22	0.845	1	0.22	57.065	64.895	33.826
10	10	40	$\lfloor 0.5n \rfloor$	10	1	1	1	1	0.998	0.894	0.534	0.288	0.839	1	0.288	32.421	43.250	18.655
10	10	40	$\lfloor 0.5n \rfloor$	50	1	1	1	1	1	0.955	0.552	0.267	0.847	1	0.267	126.972	178.203	59.322
10	10	70	$\lfloor 0.1n \rfloor$	10	1	1	0.998	1	0.993	0.916	0.55	0.163	0.828	1	0.163	2.474	2.855	2.129
10	10	70	$\lfloor 0.1n \rfloor$	50	1	1	0.997	1	0.994	0.923	0.562	0.162	0.83	1	0.162	6.802	7.603	6.094
10	10	70	$\lfloor 0.3n \rfloor$	10	1	1	1	1	1	0.951	0.562	0.224	0.842	1	0.224	15.567	17.461	10.675
10	10	70	$\lfloor 0.3n \rfloor$	50	1	1	1	1	1	0.957	0.604	0.218	0.847	1	0.218	56.963	64.597	33.589
10	10	70	$\lfloor 0.5n \rfloor$	10	1	1	1	1	1	0.908	0.549	0.288	0.843	1	0.288	33.021	43.464	19.996
10	10	70	$\lfloor 0.5n \rfloor$	50	1	1	1	1	1	0.958	0.586	0.264	0.851	1	0.264	125.699	177.726	58.092

Table A.7: Experiments to adjust parameters of *MOSpecG-mod* to large-sized community networks - part 2.

$N\mathcal{G}$	$N\mathcal{P}$	$N\mathcal{O}$	p	IT	0.1	0.2	0.3	0.4	0.5	0.6	0.7	0.8	AVG	MAX	MIN	AVG	MAX	MIN
	Parameters							μ						NMI			Time (s)	
50	5	10	⌊0.1n⌋	10	0.932	0.926	0.915	0.881	0.779	0.592	0.358	0.186	0.696	0.932	0.186	4.224	4.759	3.710
50	5	10	⌊0.1n⌋	50	0.93	0.931	0.914	0.893	0.792	0.591	0.366	0.181	0.7	0.931	0.181	14.998	16.184	13.520
50	5	10	⌊0.3n⌋	10	0.844	0.793	0.753	0.684	0.626	0.524	0.423	0.325	0.622	0.844	0.325	31.105	35.189	19.478
50	5	10	⌊0.3n⌋	50	0.843	0.789	0.754	0.702	0.622	0.509	0.426	0.322	0.621	0.843	0.322	135.181	153.748	76.298
50	5	10	⌊0.5n⌋	10	0.808	0.756	0.718	0.666	0.609	0.528	0.479	0.412	0.622	0.808	0.412	67.111	93.828	33.073
50	5	10	⌊0.5n⌋	50	0.807	0.745	0.716	0.669	0.602	0.532	0.478	0.409	0.62	0.807	0.409	301.115	428.742	131.385
50	5	40	⌊0.1n⌋	10	1	0.998	1	0.998	0.99	0.911	0.547	0.163	0.826	1	0.163	4.087	4.635	3.712
50	5	40	⌊0.1n⌋	50	1	0.999	0.997	0.997	0.99	0.921	0.579	0.158	0.83	1	0.158	14.683	16.143	13.091
50	5	40	⌊0.3n⌋	10	1	1	1	1	1	0.937	0.563	0.23	0.841	1	0.23	31.282	34.875	20.368
50	5	40	⌊0.3n⌋	50	1	1	1	1	1	0.974	0.641	0.201	0.852	1	0.201	134.389	153.39	75.743
50	5	40	⌊0.5n⌋	10	1	1	1	1	0.999	0.937	0.529	0.301	0.846	1	0.301	67.367	94.62	32.814
50	5	40	⌊0.5n⌋	50	1	1	1	1	1	0.985	0.644	0.229	0.857	1	0.229	300.352	428.367	131.312
50	5	70	⌊0.1n⌋	10	1	0.999	0.997	1	0.99	0.918	0.527	0.162	0.824	1	0.162	4.027	4.447	3.703
50	5	70	⌊0.1n⌋	50	1	1	1	1	0.989	0.922	0.58	0.164	0.832	1	0.164	14.66	16.232	13.067
50	5	70	⌊0.3n⌋	10	1	1	1	1	1	0.936	0.535	0.226	0.837	1	0.226	30.878	34.783	19.224
50	5	70	⌊0.3n⌋	50	1	1	1	1	1	0.976	0.656	0.204	0.855	1	0.204	135.167	155.312	75.903
50	5	70	⌊0.5n⌋	10	0.999	1	1	1	1	0.927	0.541	0.293	0.845	1	0.293	67.147	93.092	33.515
50	5	70	⌊0.5n⌋	50	1	1	1	1	1	0.981	0.643	0.233	0.857	1	0.233	299.192	427.945	130.060
50	10	10	⌊0.1n⌋	10	1	1	1	1	0.993	0.911	0.545	0.15	0.825	1	0.150	6.723	7.645	5.909
50	10	10	⌊0.1n⌋	50	1	1	1	1	0.992	0.921	0.584	0.149	0.831	1	0.149	28.019	30.141	25.396
50	10	10	⌊0.3n⌋	10	1	1	1	1	1	0.936	0.56	0.228	0.841	1	0.228	56.882	64.804	33.292
50	10	10	⌊0.3n⌋	50	1	1	1	1	1	0.964	0.626	0.201	0.849	1	0.201	264.048	302.558	146.594
50	10	10	⌊0.5n⌋	10	1	1	1	1	0.996	0.907	0.534	0.292	0.841	1	0.292	125.298	176.993	57.505
50	10	10	⌊0.5n⌋	50	1	1	1	1	1	0.982	0.646	0.24	0.859	1	0.24	591.621	848.621	253.270
50	10	40	⌊0.1n⌋	10	1	1	0.999	1	0.992	0.919	0.55	0.159	0.827	1	0.159	6.754	7.557	6.089
50	10	40	⌊0.1n⌋	50	1	1	1	1	0.994	0.924	0.574	0.157	0.831	1	0.157	27.789	30.046	25.031
50	10	40	⌊0.3n⌋	10	1	1	1	1	1	0.943	0.574	0.222	0.842	1	0.222	56.830	64.593	33.236
50	10	40	⌊0.3n⌋	50	1	1	1	1	1	0.978	0.657	0.202	0.855	1	0.202	264.380	304.638	146.540
50	10	40	⌊0.5n⌋	10	1	1	1	1	1	0.915	0.529	0.289	0.842	1	0.289	125.720	176.901	58.693
50	10	40	⌊0.5n⌋	50	1	1	1	1	1	0.985	0.638	0.228	0.856	1	0.228	590.405	846.248	251.792
50	10	70	⌊0.1n⌋	10	1	1	1	1	0.994	0.923	0.554	0.153	0.828	1	0.153	6.721	7.487	5.951
50	10	70	⌊0.1n⌋	50	1	1	1	1	0.994	0.917	0.574	0.16	0.831	1	0.160	27.836	30.097	25.076
50	10	70	⌊0.3n⌋	10	1	1	1	1	1	0.955	0.574	0.213	0.843	1	0.213	56.987	64.592	33.512
50	10	70	⌊0.3n⌋	50	1	1	1	1	1	0.97	0.657	0.206	0.854	1	0.206	267.935	310.419	146.354
50	10	70	⌊0.5n⌋	10	1	1	1	1	1	0.943	0.555	0.29	0.849	1	0.290	127.842	177.911	57.568
50	10	70	⌊0.5n⌋	50	1	1	1	1	1	0.987	0.636	0.229	0.857	1	0.229	605.327	927.813	255.824

Table A.8: Experiments to adjust parameters of *MOSpecG-mod* to real networks - part 1.

Parameters					Karate		Dolphins		Polbooks		Football	
$N\mathcal{G}$	$N\mathcal{P}$	$N\mathcal{O}$	p	IT	NMI	Time (s)	NMI	Time (s)	NMI	Time (s)	NMI	Time (s)
10	5	10	$\lfloor 0.1n \rfloor$	10	0.828	0.002	0.429	0.007	0.446	0.028	0.83	0.039
10	5	10	$\lfloor 0.1n \rfloor$	50	0.795	0.005	0.448	0.022	0.441	0.073	0.828	0.074
10	5	10	$\lfloor 0.3n \rfloor$	10	0.589	0.014	0.445	0.017	0.409	0.042	0.831	0.058
10	5	10	$\lfloor 0.3n \rfloor$	50	0.55	0.014	0.44	0.023	0.413	0.066	0.834	0.091
10	5	10	$\lfloor 0.5n \rfloor$	10	0.489	0.012	0.42	0.012	0.419	0.042	0.829	0.06
10	5	10	$\lfloor 0.5n \rfloor$	50	0.54	0.012	0.439	0.027	0.426	0.081	0.828	0.124
10	5	40	$\lfloor 0.1n \rfloor$	10	1	0.002	0.541	0.005	0.454	0.018	0.863	0.017
10	5	40	$\lfloor 0.1n \rfloor$	50	1	0.004	0.57	0.01	0.477	0.028	0.866	0.039
10	5	40	$\lfloor 0.3n \rfloor$	10	0.699	0.011	0.523	0.013	0.524	0.024	0.89	0.041
10	5	40	$\lfloor 0.3n \rfloor$	50	0.675	0.013	0.533	0.029	0.527	0.056	0.875	0.079
10	5	40	$\lfloor 0.5n \rfloor$	10	0.675	0.011	0.534	0.014	0.503	0.033	0.897	0.053
10	5	40	$\lfloor 0.5n \rfloor$	50	0.699	0.013	0.573	0.029	0.536	0.097	0.892	0.121
10	5	70	$\lfloor 0.1n \rfloor$	10	1	0.002	0.561	0.004	0.456	0.014	0.865	0.02
10	5	70	$\lfloor 0.1n \rfloor$	50	1	0.004	0.561	0.01	0.463	0.026	0.852	0.031
10	5	70	$\lfloor 0.3n \rfloor$	10	0.699	0.015	0.53	0.015	0.498	0.038	0.872	0.043
10	5	70	$\lfloor 0.3n \rfloor$	50	0.699	0.016	0.529	0.025	0.524	0.06	0.891	0.082
10	5	70	$\lfloor 0.5n \rfloor$	10	0.7	0.011	0.554	0.012	0.5	0.049	0.903	0.049
10	5	70	$\lfloor 0.5n \rfloor$	50	0.697	0.015	0.574	0.037	0.508	0.09	0.888	0.124
10	10	10	$\lfloor 0.1n \rfloor$	10	1	0.002	0.56	0.005	0.457	0.02	0.867	0.028
10	10	10	$\lfloor 0.1n \rfloor$	50	1	0.006	0.561	0.017	0.477	0.05	0.866	0.069
10	10	10	$\lfloor 0.3n \rfloor$	10	0.699	0.01	0.52	0.02	0.542	0.043	0.883	0.051
10	10	10	$\lfloor 0.3n \rfloor$	50	0.699	0.017	0.533	0.043	0.541	0.086	0.885	0.128
10	10	10	$\lfloor 0.5n \rfloor$	10	0.699	0.013	0.58	0.017	0.533	0.044	0.895	0.102
10	10	10	$\lfloor 0.5n \rfloor$	50	0.699	0.019	0.588	0.049	0.524	0.125	0.892	0.187
10	10	40	$\lfloor 0.1n \rfloor$	10	1	0.003	0.561	0.006	0.47	0.024	0.88	0.024
10	10	40	$\lfloor 0.1n \rfloor$	50	1	0.007	0.561	0.022	0.486	0.049	0.868	0.074
10	10	40	$\lfloor 0.3n \rfloor$	10	0.699	0.011	0.524	0.018	0.533	0.037	0.903	0.054
10	10	40	$\lfloor 0.3n \rfloor$	50	0.699	0.017	0.533	0.034	0.527	0.086	0.884	0.123
10	10	40	$\lfloor 0.5n \rfloor$	10	0.699	0.013	0.572	0.021	0.515	0.062	0.892	0.08
10	10	40	$\lfloor 0.5n \rfloor$	50	0.699	0.018	0.587	0.051	0.547	0.135	0.9	0.181
10	10	70	$\lfloor 0.1n \rfloor$	10	1	0.003	0.581	0.006	0.477	0.013	0.862	0.02
10	10	70	$\lfloor 0.1n \rfloor$	50	1	0.008	0.57	0.016	0.473	0.043	0.87	0.06
10	10	70	$\lfloor 0.3n \rfloor$	10	0.699	0.008	0.542	0.014	0.556	0.026	0.879	0.04
10	10	70	$\lfloor 0.3n \rfloor$	50	0.699	0.008	0.533	0.034	0.541	0.084	0.884	0.125
10	10	70	$\lfloor 0.5n \rfloor$	10	0.7	0.009	0.568	0.012	0.515	0.047	0.89	0.059
10	10	70	$\lfloor 0.5n \rfloor$	50	0.699	0.01	0.587	0.037	0.524	0.121	0.887	0.167

Table A.9: Experiments to adjust parameters of *MOSpecG-mod* to real networks - part 2.

Parameters					Karate		Dolphins		Polbooks		Football	
$N\mathcal{G}$	$N\mathcal{P}$	$N\mathcal{O}$	p	IT	NMI	Time (s)	NMI	Time (s)	NMI	Time (s)	NMI	Time (s)
50	5	10	$\lfloor 0.1n \rfloor$	10	0.806	0.006	0.428	0.01	0.442	0.025	0.846	0.04
50	5	10	$\lfloor 0.1n \rfloor$	50	0.808	0.014	0.425	0.044	0.44	0.095	0.844	0.137
50	5	10	$\lfloor 0.3n \rfloor$	10	0.537	0.019	0.462	0.039	0.431	0.061	0.845	0.106
50	5	10	$\lfloor 0.3n \rfloor$	50	0.507	0.04	0.442	0.091	0.423	0.19	0.833	0.254
50	5	10	$\lfloor 0.5n \rfloor$	10	0.59	0.025	0.426	0.035	0.411	0.108	0.844	0.162
50	5	10	$\lfloor 0.5n \rfloor$	50	0.548	0.038	0.456	0.104	0.403	0.265	0.833	0.391
50	5	40	$\lfloor 0.1n \rfloor$	10	1	0.008	0.581	0.015	0.47	0.034	0.855	0.082
50	5	40	$\lfloor 0.1n \rfloor$	50	1	0.031	0.581	0.079	0.475	0.111	0.882	0.25
50	5	40	$\lfloor 0.3n \rfloor$	10	0.699	0.032	0.52	0.055	0.529	0.128	0.873	0.176
50	5	40	$\lfloor 0.3n \rfloor$	50	0.699	0.053	0.533	0.121	0.538	0.272	0.885	0.36
50	5	40	$\lfloor 0.5n \rfloor$	10	0.675	0.022	0.546	0.046	0.508	0.185	0.888	0.216
50	5	40	$\lfloor 0.5n \rfloor$	50	0.699	0.077	0.575	0.156	0.531	0.389	0.89	0.559
50	5	70	$\lfloor 0.1n \rfloor$	10	1	0.009	0.571	0.029	0.472	0.052	0.882	0.084
50	5	70	$\lfloor 0.1n \rfloor$	50	1	0.029	0.581	0.064	0.474	0.147	0.866	0.211
50	5	70	$\lfloor 0.3n \rfloor$	10	0.71	0.016	0.532	0.052	0.525	0.137	0.888	0.157
50	5	70	$\lfloor 0.3n \rfloor$	50	0.699	0.049	0.533	0.114	0.538	0.291	0.889	0.378
50	5	70	$\lfloor 0.5n \rfloor$	10	0.698	0.032	0.57	0.049	0.504	0.132	0.89	0.215
50	5	70	$\lfloor 0.5n \rfloor$	50	0.699	0.056	0.586	0.159	0.537	0.395	0.891	0.565
50	10	10	$\lfloor 0.1n \rfloor$	10	1	0.009	0.581	0.028	0.464	0.076	0.885	0.126
50	10	10	$\lfloor 0.1n \rfloor$	50	1	0.097	0.581	0.121	0.486	0.24	0.875	0.325
50	10	10	$\lfloor 0.3n \rfloor$	10	0.699	0.031	0.536	0.077	0.555	0.194	0.891	0.198
50	10	10	$\lfloor 0.3n \rfloor$	50	0.699	0.077	0.533	0.192	0.546	0.447	0.894	0.652
50	10	10	$\lfloor 0.5n \rfloor$	10	0.699	0.033	0.58	0.078	0.536	0.264	0.904	0.284
50	10	10	$\lfloor 0.5n \rfloor$	50	0.699	0.088	0.588	0.237	0.548	0.621	0.899	0.926
50	10	40	$\lfloor 0.1n \rfloor$	10	1	0.011	0.581	0.036	0.476	0.095	0.873	0.128
50	10	40	$\lfloor 0.1n \rfloor$	50	1	0.076	0.581	0.115	0.497	0.24	0.875	0.297
50	10	40	$\lfloor 0.3n \rfloor$	10	0.699	0.034	0.529	0.07	0.533	0.17	0.904	0.239
50	10	40	$\lfloor 0.3n \rfloor$	50	0.699	0.085	0.533	0.19	0.543	0.408	0.894	0.646
50	10	40	$\lfloor 0.5n \rfloor$	10	0.699	0.027	0.58	0.094	0.52	0.278	0.893	0.275
50	10	40	$\lfloor 0.5n \rfloor$	50	0.699	0.118	0.588	0.209	0.533	0.581	0.89	0.803
50	10	70	$\lfloor 0.1n \rfloor$	10	1	0.009	0.581	0.026	0.479	0.054	0.879	0.083
50	10	70	$\lfloor 0.1n \rfloor$	50	1	0.031	0.581	0.131	0.481	0.246	0.88	0.245
50	10	70	$\lfloor 0.3n \rfloor$	10	0.699	0.03	0.532	0.058	0.531	0.189	0.878	0.195
50	10	70	$\lfloor 0.3n \rfloor$	50	0.699	0.073	0.533	0.129	0.547	0.378	0.885	0.588
50	10	70	$\lfloor 0.5n \rfloor$	10	0.699	0.028	0.568	0.06	0.521	0.293	0.896	0.218
50	10	70	$\lfloor 0.5n \rfloor$	50	0.699	0.072	0.587	0.262	0.537	0.526	0.894	0.803

Table A.10: Pearson correlation coefficients between *MOSpecG-mod* parameters and results for small-sized networks.

Parameters	NMI value achieved over each μ								Time (s)		
	0.1	0.2	0.3	0.4	0.5	0.6	0.7	0.8	AVG	MAX	MIN
$N\mathcal{G}$	0.004	0.011	0.001	-0.004	0	0.006	0.056	-0.016	0.397	0.376	0.428
$N\mathcal{P}$	0.463	0.456	0.441	0.435	0.44	0.438	0.381	-0.109	0.198	0.188	0.215
$N\mathcal{O}$	0.518	0.522	0.52	0.51	0.523	0.531	0.463	-0.157	-0.002	0	-0.009
p	-0.076	-0.041	0.022	0.025	0.038	0.096	0.467	0.903	0.492	0.5	0.489
IT	-0.01	0.004	0.007	0.005	0.002	0.014	0.124	-0.029	0.403	0.38	0.444

Table A.11: Pearson correlation coefficients between *MOSpecG-mod* parameters and results for large-sized networks.

Parameters	NMI value achieved over each μ								Time (s)		
	0.1	0.2	0.3	0.4	0.5	0.6	0.7	0.8	AVG	MAX	MIN
$N\mathcal{G}$	0.007	-0.002	0.003	-0.001	0.002	0.05	0.175	-0.055	0.393	0.372	0.420
$N\mathcal{P}$	0.416	0.407	0.408	0.411	0.434	0.443	0.371	-0.225	0.197	0.189	0.209
$N\mathcal{O}$	0.508	0.497	0.496	0.503	0.531	0.557	0.49	-0.286	0	0.005	-0.002
p	-0.145	-0.162	-0.155	-0.149	-0.083	0.009	0.197	0.797	0.492	0.496	0.478
IT	0.003	-0.004	-0.003	0.005	0.005	0.095	0.34	-0.119	0.398	0.376	0.428

Table A.12: Pearson correlation coefficients between the parameters and results obtained by *MOSpecG-mod* for real networks.

Parameters	Karate		Dolphins		Polbooks		Football	
	NMI	Time (s)	NMI	Time (s)	NMI	Time (s)	NMI	Time (s)
$N\mathcal{G}$	0.034	0.582	0.154	0.605	0.150	0.614	0.211	0.569
$N\mathcal{P}$	0.186	0.292	0.499	0.315	0.476	0.337	0.507	0.294
$N\mathcal{O}$	0.181	-0.071	0.414	-0.006	0.276	0.001	0.313	-0.026
p	-0.803	0.245	0.021	0.302	0.406	0.411	0.374	0.377
IT	-0.006	0.487	0.077	0.509	0.115	0.436	-0.040	0.485

Table A.13: Parameter-tuning experiments for *SpecG-EC* with small-sized community networks.

Parameters		μ								NMI			Time (s)		
$N\mathcal{F}$	τ	0.1	0.2	0.3	0.4	0.5	0.6	0.7	0.8	AVG	MAX	MIN	AVG	MAX	MIN
6	0.1	0.339	0.296	0.007	0.222	0.097	0	0	0.001	0.12	0.339	0	3.189	3.637	2.030
6	0.25	0.905	0.889	0.869	0.733	0.008	0.007	0	0	0.426	0.905	0	3.354	4.165	1.855
6	0.5	0.968	0.96	0.954	0.927	0.833	0.588	0.011	0.01	0.656	0.968	0.01	3.381	4.068	2.283
6	0.75	0.982	0.972	0.976	0.977	0.973	0.97	0.842	0.397	0.886	0.982	0.397	4.434	7.283	3.163
11	0.1	0.918	0.916	0.912	0.9	0.73	0	0	0	0.547	0.918	0	3.825	4.978	2.999
11	0.25	0.966	0.958	0.953	0.961	0.958	0.878	0.33	0.032	0.755	0.966	0.032	3.403	3.614	3.146
11	0.5	0.98	0.978	0.974	0.972	0.965	0.962	0.822	0.284	0.867	0.98	0.284	4.903	6.938	4.029
11	0.75	0.982	0.974	0.976	0.976	0.973	0.961	0.871	0.402	0.889	0.982	0.402	5.251	8.905	3.247

Table A.14: Parameter-tuning experiments for *SpecG-EC* with large-sized community networks.

Parameters		μ								NMI			Time (s)		
$N\mathcal{F}$	τ	0.1	0.2	0.3	0.4	0.5	0.6	0.7	0.8	AVG	MAX	MIN	AVG	MAX	MIN
6	0.1	0.783	0.815	0.765	0.42	0	0.002	0	0	0.348	0.815	0	3.56	4.313	2.825
6	0.25	0.947	0.941	0.953	0.705	0.005	0	0	0	0.444	0.953	0	3.587	4.446	2.094
6	0.5	0.986	0.997	0.988	0.965	0.771	0.112	0.006	0.006	0.604	0.997	0.006	4.059	5.211	3.152
6	0.75	0.982	0.994	0.985	0.989	0.976	0.903	0.575	0.196	0.825	0.994	0.196	5.379	9.376	3.570
11	0.1	0.957	0.939	0.942	0.915	0.811	0	0	0	0.571	0.957	0	3.794	4.447	3.218
11	0.25	0.989	0.986	0.991	0.986	0.963	0.693	0.106	0.011	0.716	0.991	0.011	2.787	3.276	2.360
11	0.5	0.992	0.985	0.984	0.987	0.978	0.917	0.523	0.108	0.809	0.992	0.108	4.349	7.4	3.007
11	0.75	0.98	0.99	0.979	0.991	0.979	0.931	0.594	0.201	0.831	0.991	0.201	5.54	9.455	3.908

Table A.15: Parameter-tuning experiments for *SpecG-EC* with real networks.

Parameters		Karate		Dolphins		Polbooks		Football	
$N\mathcal{F}$	τ	NMI	Time (s)	NMI	Time (s)	NMI	Time (s)	NMI	Time (s)
6	0.1	1	0.012	0.889	0.028	0.432	0.079	0.327	0.115
6	0.25	1	0.013	0.889	0.028	0.546	0.079	0.55	0.123
6	0.5	1	0.013	0.889	0.035	0.552	0.084	0.748	0.135
6	0.75	1	0.015	0.581	0.028	0.536	0.097	0.877	0.13
11	0.1	1	0.013	0.889	0.026	0.569	0.077	0.564	0.116
11	0.25	1	0.011	0.889	0.028	0.569	0.079	0.717	0.121
11	0.5	1	0.014	0.889	0.029	0.561	0.119	0.883	0.161
11	0.75	1	0.011	0.581	0.027	0.554	0.074	0.872	0.116